



Huliienko S. V., Korniyenko Y. M., Muzyka S. M., Holubka K. (2022). Simulation of reverse osmosis process: Novel approaches and development trends. *Journal of Engineering Sciences*, Vol. 9(2), pp. F6-F36, doi: 10.21272/jes.2022.9(2).f2

## Simulation of Reverse Osmosis Process: Novel Approaches and Development Trends

Huliienko S. V.<sup>1</sup>[0000-0002-9042-870X], Korniyenko Y. M.<sup>1</sup>[0000-0002-3031-6212], Muzyka S. M.<sup>1</sup>, Holubka K.<sup>2</sup>

<sup>1</sup> National Technical University of Ukraine “Igor Sikorsky Kyiv Polytechnic Institute”, 37, Peremohy Ave., 03056, Kyiv, Ukraine;

<sup>2</sup> University of Montpellier, 163, Auguste Broussonnet St., 34090, Montpellier, France

### Article info:

Submitted:

May 8, 2022

Accepted for publication:

September 9, 2022

Available online:

September 12, 2022

### \*Corresponding email:

[sergii.guliienko@gmail.com](mailto:sergii.guliienko@gmail.com)

**Abstract.** Reverse osmosis is an essential technological separation process that has a large number of practical applications. The mathematical simulation is significant for designing and determining the most effective modes of membrane equipment operation and for a deep understanding of the processes in membrane units. This paper is an attempt at systematization and generalizing the results of the investigations dedicated to reverse osmosis simulation, which was published from 2011 to 2020. The main approaches to simulation were analyzed, and the scope of use of each of them was delineated. It was defined that computational fluid dynamics was the most used technique for reverse osmosis simulation; the intensive increase in using of molecular dynamics methods was pointed out. Since these two approaches provide the deepest insight into processes, it is likely that they will further be widely used for reverse osmosis simulations. At the same time, for the simulation of the membrane plant, it is reasonable to use the models that required the simplest solutions methods. The solution-diffusion model appears to be the most effective and flexible for these purposes. Therefore, this model was widely used in considering the period. The practical problems solved using each of the considered approaches were reviewed. Moreover, the software used for the solution of the mathematical models was regarded.

**Keywords:** reverse osmosis, membrane, simulation, optimization, software.

## 1 Introduction

The pressure-driven membrane processes are widely used in many industries, including chemical, food, pharmaceutical, biotechnologies, water treatment, and environmental protection. The mathematical simulation of the process plays an essential role in designing and exploring such equipment since this technique defines the most rational design of apparatus and operation modes with a lower number of experimental investigations. However, there exists quite a significant number of approaches to the simulation. Therefore, the systematized information about types of mathematical models of pressure-driven membrane processes would help choose the simulation method for the particular process. In previous work [1], the attempt was to systematize the theoretical investigation of pressure driven membrane processes from 2000 to 2010. This work is an extension of the previous one, and the works published between 2011 and 2020 are considered there.

First of all, it should be noted that in work [1], in the waste majority of cases, it was considered the articles

published in the leading thematic journal, namely Journal of Membrane Science and Desalination by Elsevier. In contrast, the attention to the other publication was insufficient. Also, during the considered period, new thematic journals began to be issued, particularly Membranes by MDPI. Therefore, the current work analyzed the bigger number of journals and more than 1000 publications dedicated to pressure driven membrane processes simulation. The publication distribution by years is shown in Figure 1, and the distribution among the main processes is shown in Figure 2.

It can be seen from Figure 1 that despite the drop in 2017 and 2018, the number of publications stable increased, which is evident that the actuality of such kind of investigation is increased. Moreover, the trend of the increase is more clearly seen than it was in work [1]. Figure 2, in turn, shows that the most significant number of research is dedicated to the question of simulation of reverse osmosis, which is the most widely applied industrial pressure-driven membrane process. Also, a significant number of publications are dedicated to the simulation of nanofiltration (NF) and forward osmosis

(FO), which in work [1] was not considered. A lesser number of works are dedicated simulation of ultrafiltration (UF), microfiltration (MF), and also membrane bioreactors. The last ones were not considered in work [1] as a separate kind of process.

Taking into account a large number of publications in the considered period it was decided to make a review for each process separately. Correspondingly, the purpose of the current work is the analysis and generalization of the investigations dedicated to the simulation of reverse osmosis in the period from 2011 to 2020. The objectives of the research include: (1) the review and evaluation of areas for applications of the different approaches to RO simulations; (2) the comparison of the trends in developments of methods of RO simulation in the first two decades of the XXI century; (3) the analysis perspectives of the development of the RO simulation.

The distribution of the published works dedicated to RO simulation is shown in Figure 3. The represented data demonstrate that the research interest in this direction was steadily increasing.

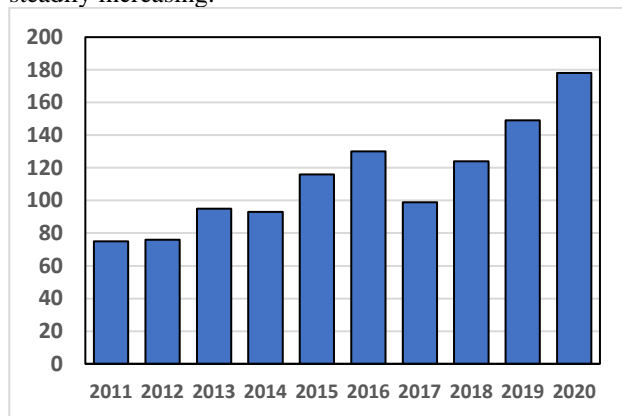


Figure 1 – The distribution of the publications selected for review by the years

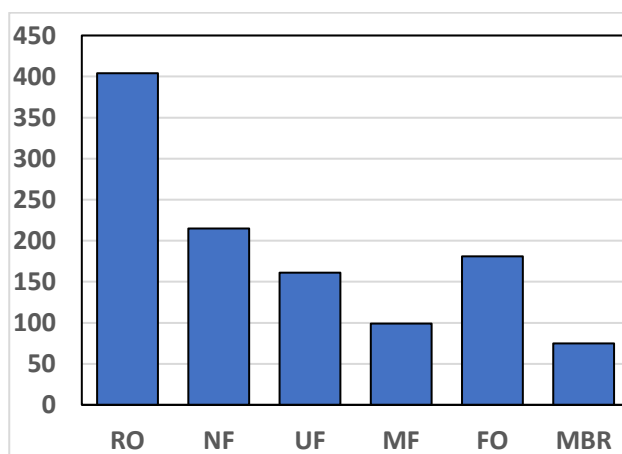


Figure 2 – The distribution the publication selected for review by the processes

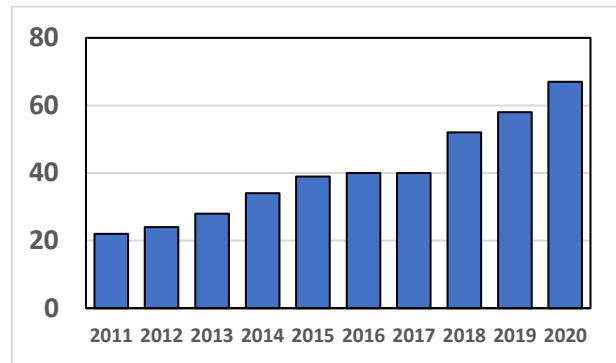


Figure 3 – The distribution of publications dedicated to the simulation of reverse osmosis by the years

As in work [1], the review does not claim comprehensiveness, however, it allows to sufficiently evaluate the main trends in the mathematical simulation of RO and the areas of application of the main approaches to the simulation.

It should be noticed that in 2011-2020 several substantial review articles were published in which the question of reverse osmosis simulation was considered. These works will be discussed below.

## 2 Research Methodology

In work [1] it was noticed that the traditional models include the following groups: irreversible thermodynamics-based models, diffusion-based models, and pore-flow-based models. The investigations with the application of computational fluid dynamics, artificial neuron networks, optimization, and economic analysis were identified as individual groups. The others approaches to the reverse osmosis simulation including semi-empirical models were also considered separately.

During 2011-2020 several reviews were published which prove the acceptability of such classifications with some corrections. In particular, in work [1] the models based on Kedem–Katchalsky equation (irreversible thermodynamics) were considered, and in work [3] detailed analysis of the irreversible thermodynamics and solution-diffusion models was made. The traditional models were also considered in the general review of RO desalination [4] and the review of the desalination processes simulation [5]. The reviewed works dedicated to the simulation with using of the computation fluids dynamics (CFD) [6-8] and molecular dynamics [9-11] were also published. Moreover, in works [12-13] it was considered both the traditional models and the molecular dynamics methods, in addition, in work [13] it was noticed that in researches until 2000 the application of the preferential sorption-capillary flow model was predominated while after 2001 the biggest progress was achieved with using of the molecular dynamic methods. The question of the RO optimization was considered in reviewed works [5, 14], and in work [15] the studies of the energy analysis of RO were revived.

In this review works the authors considered mainly modern researches, and the fraction of the works published

in the 1960s-1980s is relatively low. They significantly provide an indication of the state of art in the reverse osmosis mathematical simulation according to the individual approaches, however, no one of them did not consider all main approaches together. For example, in generalized works [12-13] the simulation using the CFD methods was not considered, and the attention to the artificial neuron networks in the reviews is almost absent. Therefore, such a review like the current work would be useful for the generalized understanding of the RO simulation and the trends of the mathematical modeling of RO.

Taking into account the works [9-11] and work [15], it was decided that except the class of models distinguished in the previous work [1] to consider individually the molecular dynamics method and energy analysis. With this, the distribution of the approaches in chosen for the review publication is shown in Figure 4.

As in the previous period, the most number of works are dedicated to the simulation with an application of CFD and optimization methods, while the number of irreversible thermodynamics-based models and pore flow-based models is still low. It was unexpected to define the relatively high number of models based on the solution-diffusion concept.

### 3 Results

#### 3.1 Irreversible thermodynamics models

The main models of this class include the Kedem–Katchalsky and the Spiegler–Kedem model, which was used in the limited extend during 2011-2020 (Figure 5). In particular. The Kedem–Katchalsky model was considered in works [2, 16-19], the works [20-27] were dedicated to the Spiegler–Kedem model, and in works [3, 28], both models were used.

The Kedem–Katchalsky model is based on the assumption of a linear relationship between flux and potential gradient. The membrane performance, in this case, can be determined by using phenomenological coefficients [9].

The transport through the membrane of non-electrolyte binary solutions, caused by the pressure difference and also by the osmotic pressure difference, according to the Kedem–Katchalsky model can be described by the following equations [2]:

$$J_w = L_p (\Delta p - \sigma \Delta \pi) \quad (1)$$

$$J_s = \omega \Delta \pi + (1 - \sigma) \bar{c} \cdot J_w \quad (2)$$

where  $\Delta p$  is the applied pressure difference;  $\Delta \pi$  is the osmotic pressure difference;  $\bar{c}$  is the mean concentration of salt in the membrane which can be determined as mean arithmetic [2] or mean logarithm [9] value. The values  $L_p$ ,  $\sigma$  and  $\omega$  are the phenomenological constants that are concentration depended.

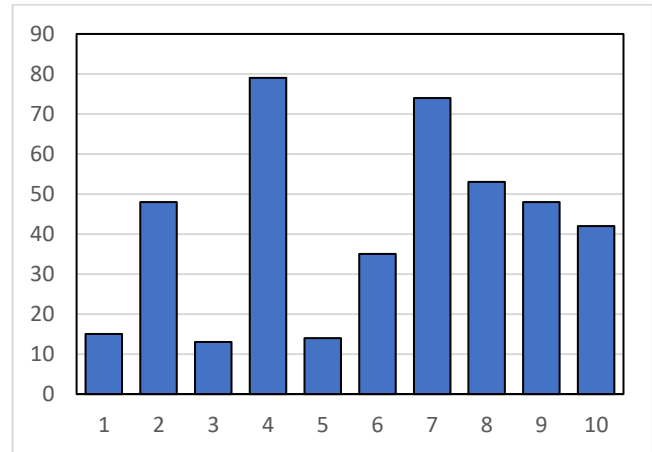


Figure 4 – The distribution of the RO models in chosen publication by classes: 1 – irreversible thermodynamics; 2 – diffusion; 3 – pore flow; 4 – computational fluid dynamics; 5 – artificial neuron networks; 6 – molecular dynamics; 7 – optimization; 8 – energy analysis; 9 – economic analysis; 10 – others models

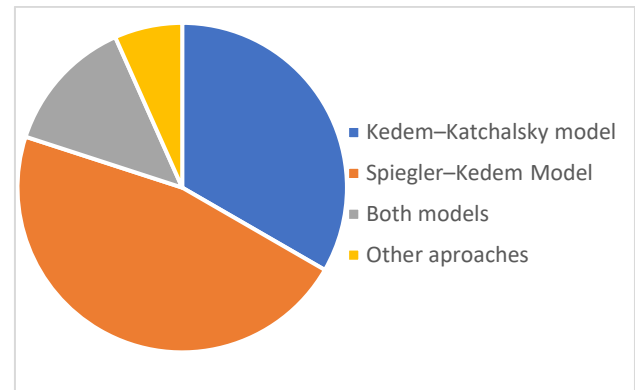


Figure 5 – The distribution of the irreversible thermodynamic based models in chosen publications

The selectivity of process can be evaluated by using of the rejection coefficient [9]:

$$R = 1 - \frac{c_3}{c_1} = 1 - \frac{J_s}{J_w c_1} \quad (3)$$

where  $c_1$  is the solute concentration in feed solution;  $c_2$  is the solute concentration in permeate.

The osmotic pressure value can be defined by the van't Hoff equation [2, 9]:

$$\Delta \pi = RT \Delta c = RT (c_2 - c_3) \quad (4)$$

where  $R$  is the universal gas constant;  $T$  is the absolute temperature;  $c_1$  is the solute concentration near the membrane surface.

$$\pi(i) = 1.19(T + 273) \sum_1^i m(i) \quad (5)$$

where  $T$  is the solution temperature;  $m(i)$  – is molar concentration of ions.

On the other hand, in work [19] the osmotic pressure of glucose solution was determined as the function of concentration:

$$\pi(c) = -RT \ln \left\{ \frac{\left[ (100 - c/M_w) - (2c/M_g) \right]}{\left[ (100 - c/M_w) - (c/M_g) \right]} \right\} \quad (6)$$

where  $R$  is the gas constant;  $T$  is the solutions temperatures;  $M_g$  is the glucose molar weight;  $M_w$  is the water molar weight.

Also, the set of the temperature and concentration dependences of osmotic pressure is represented in the work [27].

The dependences of phenomenological constants in equations (1) and (2) from the operation condition are discussed in detail in the review work [2].

The use of the Kedem–Katchalsky model in the considered period was limited and related to the simulation of the hydrogen peroxide [16, 17], the rejection of N-nitrosamines [18] and boron [28], and also for the glucose solution concentration.

The more recent Spiegler–Kedem model describe the process of the substance transport through the membrane using the differential equations in a form [24]:

$$J_w = -A \left( \frac{dp}{dx} - \sigma \frac{d\pi}{dx} \right) \quad (7)$$

$$J_s = -B \frac{dc}{dx} + (1 - \sigma) J_w \bar{c} \quad (8)$$

The rejection coefficient can be represented in a form [24]:

$$R = 1 - \frac{(K_{ic} - (D_p / RT) V_{is} (8\eta / r_p^2) \phi)}{1 - \exp(-Pe') [1 - \phi (K_{ic} - (D_p / RT) V_{is} (8\eta / r_p^2))]} \quad (9)$$

where  $K_{ic}$  is the factor of the resistance to diffusion;  $D_i$  is the diffusivity of the component  $i$  in the pores;  $R$  is the universal gas constant;  $T$  is the absolute temperature;  $V_{is}$  is the solute partial molar volume;  $\eta$  is the solution dynamic viscosity;  $r_p$  is pore radius;  $\phi$  is the volumetric factor;  $Pe'$  is modified Peclet number.

In work [3] the other relationship was proposed for the rejection coefficient calculation:

$$R_s = 1 - \frac{1 - \sigma}{1 - \sigma \exp \left[ \frac{(\sigma - 1) J_w \Delta x}{\omega^-} \right]} \quad (10)$$

where  $\sigma$  is reflection coefficient;  $\omega^-$  is the local permeation coefficient.

The osmotic pressure value is determined in the same as in the previous case. The phenomenological coefficients (7) and (8) in contrast with the Kedem–Katchalsky model do not depend on the solvent concentration [3].

The application of the Spiegler–Kedem model also was not wide. But this model was used for the analysis of phenol rejection [22], brackish [20] and seawater [25] desalination, N-nitrosamines rejection [21, 27], boron

rejection [24, 28], water purification from organic contaminant [23], and glucose concentration [24]. In works [22–23], it also noticed that the description of processes is carried out for spiral wound modules.

It also should be noticed, that the thermodynamical approach and the phenomenological equation were used in work [29]. However, the thermodynamic method were also applied for energy analysis, which will be discussed below.

However, in general, the application of the irreversible thermodynamics models, despite their relative simplicity, in considered period were limited, and the relative number substantially decreased compared with previous period, considered in work [1].

### 3.2 Diffusion based models

From Figure 4 it can be seen that in the period 2011–2020 diffusion based models were used in a quite wide range, which was unexpected, taking into account the relatively low number of publications with using this approach in the previous decade [1].

In the vast majority of cases, the solution-diffusion model was used. Its main assumption is that the skin layer is non-porous. In this case the transport of solvent and solute can be recognized as diffusion and it can be described by the equations in a form [3, 28, 30–55]:

$$J_w = A_w (\Delta p - \Delta \pi) \quad (11)$$

$$J_s = B (C_f - C_p) \quad (12)$$

where  $A_w$  is the solvent penetration constant;  $B$  is the solute penetration constant;  $\Delta p$  is the applied pressure difference;  $\Delta \pi$  is the osmotic pressure difference;  $C_f$  is the solute concentration in the feed solution;  $C_p$  is the solvent concentration in the permeate.

$$\begin{aligned} J_s &= -D_m \frac{dC_m}{dx} = \frac{D_m}{l} (D_{m0} - D_{ml}) = \\ &= \frac{D_m K_m}{l} (C_f - C_p) = B (C_f - C_p) \end{aligned} \quad (13)$$

where  $D_m$  is the solute diffusivity in membrane;  $l$  is the active layer thickness;  $C_{m0}$  is the solute concentration in membrane on the feed side;  $C_{ml}$  is the solute concentration in the membrane on the permeate side;  $K_m$  is the partition coefficient.

In general, in several works the relationships for determination of the constants in equation (11) and (12) are represented.

For example, in work [46] the solvent penetration constant was represented in a form:

$$A = \frac{D_i \cdot K_i \cdot c_{i0} \cdot V_i}{l \cdot R \cdot T} \quad (14)$$

where  $D_i$  is the solvent diffusivity;  $K_i$  is the solvent sorption coefficient;  $c_{i0}$  is the solvent concentration in the feed solution;  $V_i$  is the solvent molar volume;  $l$  is the

membrane thickness;  $T$  is the solvent temperature;  $R$  is gas constant. The similar relationship was used in work [54].

The penetration constant also can be expressed by using the membrane resistance concept [30]:

$$A = \frac{1}{R_m \cdot \mu} \quad (15)$$

where  $R_m$  is the membrane resistance;  $\mu$  is the solvent dynamic viscosity coefficient.

Although, equation (14) directly includes the temperature, in several works for taking into account this parameter influence in the RO process the others relationships were applied. For example, in work [31] for this purpose, the change in the viscosity with temperature was used. In this case, the equations for the penetration coefficients became:

$$A(T) = \frac{A_0 \cdot \mu(T_0)}{\mu(T)} \quad (16)$$

$$B(T) = \frac{B_0 (T + 273,15) \mu(T_0)}{T_0 \cdot \mu(T)} \quad (17)$$

where  $A_0$ ,  $B_0$  are the coefficient values under base temperature.

In others works, the more complex relationships were used. Thus, in work [28] following equations were proposed:

$$A_w = A_0 e^{\left(\frac{E_A}{R} \left(\frac{1}{T} - \frac{1}{298,15}\right)\right)} \left(\frac{10^{-3}}{24 \cdot 60 \cdot 60}\right) \quad (18)$$

$$B_s = B_0 e^{\left(\frac{E_{Bs}}{R} \left(\frac{1}{T} - \frac{1}{298,15}\right)\right)} \left(\frac{10^{-3}}{24 \cdot 60 \cdot 60}\right) \quad (19)$$

where  $E_A$ ,  $E_{Bs}$  are the activation energies of the solvent and solute molecules transport through the membrane;  $R$  is gas constant.

At the same time, in work [35] for water solution it was used equations in a form:

$$A_{w,T} = 9.059 \cdot 10^{-7} \left(\frac{T}{25}\right)^{0,62} \left(\frac{36.010^5 Q_f}{400}\right)^{-0,1447} \quad (20)$$

$$B_{s,i} = B_{s,i,Ref} \exp(0.098(T - T_{Ref})) \quad (21)$$

The equation (20) was also used in work [37].

In work [57] the influence of the temperature was taken into account with following relationships:

$$A_{w(T)} = A_{w(25^\circ\text{C})} \exp[0.0343(T - 25)] \text{ at } T < 25^\circ\text{C} \quad (22)$$

$$A_{w(T)} = A_{w(25^\circ\text{C})} \exp[0.0307(T - 25)] \text{ at } T > 25^\circ\text{C} \quad (23)$$

$$B_{s(T)} = B_{s(25^\circ\text{C})} (1 + 0.08(T - 25)) \text{ at } T < 25^\circ\text{C} \quad (24)$$

$$B_{s(T)} = B_{s(25^\circ\text{C})} (1 + 0.05(T - 25)) \text{ at } T > 25^\circ\text{C} \quad (25)$$

The influence of the temperature was taken into account with using of the temperature correction factor. Thus, in work [58] the following equation was used:

$$A_{w(T)} = A_{w(25^\circ\text{C})} \cdot TFC \cdot F_f \quad (26)$$

where  $A_{w(T)}$  is the penetration coefficient under base temperature ( $25^\circ\text{C}$ );  $TFC$  is the temperature correction factor;  $F_f$  is the fouling factor.

The analogical relationships were used in works [59-60], and in work [43] the more detailed form was applied:

$$J_w = A \cdot TFC \cdot FF \cdot \left[ \left( P_f - P_p - \frac{\Delta P_f}{2} \right) - (\pi_w - \pi_p) \right] \cdot E + 6 \quad (27)$$

Also, in work [43] the relationships for the temperature correction factor were proposed:

$$TFC_p = \exp[0.0343(T - 25)] < 25^\circ\text{C} \quad (28)$$

$$TFC_p = \exp[0.0307(T - 25)] > 25^\circ\text{C} \quad (29)$$

In work [20] the long-term performance of RO plant and for the changes of the penetration coefficient in time the following relationship was proposed:

$$A_n = \delta_1 \cdot e^{-\frac{t}{\tau_1} \cdot k_{fp}} + \delta_2 \cdot e^{-\frac{t}{\tau_2} \cdot k_{fp}} \quad (30)$$

Also, in work [49] except the temperature impact the influence of pressure were taken into account with following equations:

$$A_w = A_{w_0} \exp\left(\alpha_1 \frac{T_1 - 273}{273} - \alpha_2 (P_f - P_d)\right) \quad (31)$$

$$B_s = S_{s_0} \exp\left(\beta_1 \frac{T - 273}{273}\right) \quad (32)$$

Obviously, all represented relationships have a limited range of applicability, and the condition of the validity of the equations should be checked in the corresponding publications.

The osmotic pressure values can be calculated in the same way as in the case of irreversible thermodynamics (equations (4) through (6)), and also in some works, the other methods of this parameter calculation were considered.

For example, in work [61] the van't Hoff equation were written in a form:

$$\pi = \frac{i \cdot \mathfrak{R}}{M \cdot 10^5} \cdot T \cdot C \quad (33)$$

At the same time, in work [48] the following relationship was proposed:

$$\Delta\pi = RT \left( \frac{J_s}{B_s} \right) \quad (34)$$

Also, the empirical temperature and concentration dependences for several substances are represented in works [35, 38, 55, 59].

For the evaluation of the selectivity both the rejection coefficient (equation (4)) and the solvent concentration in permeate were used.

For the rejection calculation were proposed following relationships:

in work [38]:

$$R_i = \left[ 1 + \frac{AC_{wp}}{B(\Delta p - \Delta \pi)} \right]^{-1} \quad (35)$$

where  $C_w$  is the water concentration in permeate. in work [47]:

$$R = \frac{A(\Delta p - \Delta \pi)}{A(\Delta p - \Delta \pi) + B} \quad (36)$$

Also, the relationship between the rejection coefficient and other parameters can be represented in a form [41]:

$$B = \frac{(1-R)J_w}{R} \quad (37)$$

or [54]:

$$\frac{1}{R} = B \frac{1}{J_w} + 1 \quad (38)$$

Also, the relationships for the solute concentration in permeate were proposed. In work [38] the following equation was used:

$$C_p = \frac{C_f B}{B + \frac{J_w}{\exp(J_w/k)}} \quad (39)$$

where  $k$  is the mass transfer coefficient.

A similar form of equation was applied in works [40], [48], and [53]. At the same time, in work [59], the temperature correction factor and fouling factor and with the accounting of them, the equation for the solvent concentration in permeate calculations became:

$$C_p = B \cdot FF \cdot TCF \cdot \frac{1}{J_w} \left( \frac{C_f \cdot (1 + CF)}{2} \right) \quad (40)$$

where  $CF$  is the concentration factor.

For more accurate analysis of the process the solution-diffusion model was complemented. In particular, in works [33-35, 49, 53, 56] during the RO process simulation the concentration polarization was taken into account (mainly by application of the film model). Moreover, the model was complemented by the material balance [49, 53, 55, 62], the optimization methods [35, 45, 61, 63], unsteady-state conditions [32], and by the fouling impact [39]. Also, in work [64] for the description of the processes in spiral wound membrane module the cylindrical coordinate system was used.

The solution-diffusion model was primarily used for the description of the water purification [30, 33, 36, 38, 47, 50, 64, 65], including sea water [25, 40, 41, 43, 49, 52, 55, 57, 61, 66] and brackish water [20, 31, 42, 45, 58, 59, 60, 65] desalination, and also the wastewater treatment [30, 48, 51, 53-54, 56, 67]. Also, with using of this model it was described the processes of the removal of zinc [32], boron [28, 52], chlorophenol [36, 38], N-nitrosodimethylamine [38, 63], weak acids [25], and ammonia compounds [51, 54], apple juice concentration [35, 37], and also for the membrane characterization [46]. The solution-diffusion model was also widely used for the analysis of the hybrid membrane systems performance [31, 41, 42-43, 48, 55, 57, 61, 65, 69-70]. In most cases, the processes were analyzed in the spiral wound membrane modules [33, 34-35, 37, 39, 58-60, 64, 68], the hollow fiber modules [62] and laboratory cells were also considered.

For the mathematical solutions, the most often used software includes MATLAB [32, 36, 52, 60], ROSA [39], and the programming language C++ [36].

The other models of this class were used much less often. Thus, the solution-diffusion-imperfection model was considered in works [71, 72], and the extended solution diffusion model was applied in work [72].

The solution-diffusion-imperfection model takes into account the possibility of the convective transport of substances through possible pores (imperfections) in the membrane active layer. In this case, the equations for the calculation of the solvent and solute fluxes will be written in a form [71]:

$$J_w = A(\Delta p - \Delta \pi) + L \Delta p \quad (41)$$

$$J_s = B(C_f - C_p) + L \Delta p C_f \quad (42)$$

where  $L$  is the leakage factor.

The rejection coefficient can be calculated by the equation [72]:

$$R = \left[ 1 + \left( \frac{B}{A} \right) \left( \frac{1}{\Delta p - \Delta \pi} \right) + \left( \frac{L}{A} \right) \left( \frac{\Delta p}{\Delta p - \Delta \pi} \right) \right]^{-1} \quad (43)$$

The extended solution-diffusion model takes into account the influence of the applied pressure on the solute transport, which was not considered in the classical solution-diffusion model. In this case, the equations become [72]:

$$J_w = A(\Delta p - \Delta \pi) \quad (44)$$

$$J_s = B(C_f - C_p) + L_{sp} \Delta p \quad (45)$$

here  $L_{sp}$  is the phenomenological coefficient.

The rejection coefficient can be calculated by the equation [72]:

$$\frac{1}{R} \left[ 1 - \frac{L_{sp}}{C_f A} \left( 1 - \frac{\Delta \pi}{\Delta p} \right) \right] = 1 + \frac{K_s D_s}{A(\Delta p - \Delta \pi)} \quad (46)$$

The unexpected wide range of the solution diffusion models applications in the considered period is probably related to its relative simplicity, because of what there is no necessity for the application of the complex computational techniques, and also the convenience of the model for the hybrid system analysis and the model-based optimization. It should be noticed that the significant contribution in this field was done by one research group [3, 34-38, 57-58, 63]. At the same time, the solution-diffusion-imperfection model and the extended solution diffusion model do not have these advantages, therefore, as in the previous period, they were applied in a limited range.

### 3.3 Pore flow based models

As in the previous period [1], the models of this class were used rarely, yielding to the computational fluid dynamics methods. Thus, among the large number of publications dedicated to the RO simulation the models which directly considered the pore flow are mentioned in less than 5% of cases. In most cases, the preferentially sorption pore flow model (also known as Kimura–Sourirajan model) was considered. Also, the surface force-pore flow model and some other approaches were applied (Figure 6).

Unlike the solution diffusion model, the models of this class consider the active layer as porous, and the transport is carried out by both diffusion and convection [1].

The preferentially sorption pore flow model describes the solute and solvent fluxes by the equations in a form [73]:

$$J_w = A_w (\Delta p - \Delta \pi) \quad (47)$$

$$J_s = B_s (C_m - C_p) \quad (48)$$

Such equations have a similar form to solution-diffusion models, which also can be seen in works [46, 74-75]. However, as mentioned in the previous review [1], the principal difference is in the nature of the transport coefficients, which are determined by the different conceptions of the active layer structure. Unfortunately, due to the low number of publications in the considered period, the making of a detailed review of the parameters of the preferentially sorption pore flow model does not seem possible.

For the evaluation of the selectivity the concentration in permeate may be used. It can be calculated by the equation [73-75]:

$$J_s = B_s (C_m - C_p) \quad (49)$$

Also, in work [73], the recovery ratio, which was determined as the permeate and feed ratio, was calculated:

$$R = \frac{Q_p}{Q_f} \cdot 100\% \quad (49)$$

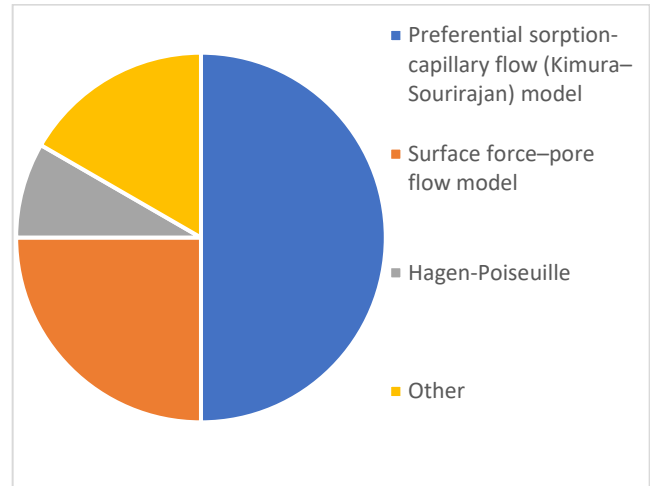


Figure 6 – The distribution of the pore flow based model in chosen publications

This model was complemented by the balance equations [73] and the optimization methods [74-75]. It was primarily used for the description of seawater desalination [74-76] and industrial effluent purification [73, 77], and also for the determinations of the characteristics and internal structure of the membrane [46]. This model was also used for the analysis of the hybrid system [76].

Also, in a few works, the surface force-pore flow model was found. This model considers the separate pore, which dimensions are characterized by the dimensionless coordinates [78-79]:

$$\rho = \frac{r}{R_w} \quad (51)$$

$$\zeta = \frac{z}{\tau} \quad (52)$$

where  $r$  is the cylindrical coordinate perpendicular to the pore wall;  $R_w$  is the pore radius;  $z$  is the cylindrical coordinate parallel to the pore axis;  $\tau$  is the average pore length.

Taking this into account, the differential equation describing the velocity profile in pores can be written in a form [78-79]:

$$\left[ \frac{d^2 \alpha(\rho)}{d\rho^2} + \frac{1}{\rho} \frac{d\alpha(\rho)}{d\rho} \right] + \frac{1}{\beta_1} \left[ \frac{\Delta P}{\pi_2} - \frac{\pi_2 \sigma_2(\rho) - \pi_3 \sigma_3(\rho)}{\pi_2} \right] - \frac{1}{\beta_1} \left( 1 - \frac{1}{b(\rho)} \right) [\alpha(\rho) + \omega(\rho)] \times \left[ 1 + \frac{1 - \left( \frac{\pi_3}{\pi_2} \right) k \cdot \rho}{\exp[\alpha(\rho) - \omega(\rho)] - 1} \right] \exp(-\Phi(\rho, 0)) = 0 \quad (53)$$

The physical meaning of the parameters in the equation (51) is described in detail in works [78-79].

The boundary conditions herewith are following [78-79]:

$$\alpha(\rho) = 0 \quad \text{at} \quad \rho = 1 \quad (54)$$

$$\frac{d\alpha(\rho)}{d\rho} = 0 \quad \text{at} \quad \rho = 0 \quad (55)$$

The solution of the equation (51) allows to represent the solvent and solute fluxes in a form [78-79]:

$$N_A = \frac{2}{X_{AB}} \left( \frac{\varepsilon}{\tau} \right) \times \int_0^{1-\lambda} \left[ \frac{\alpha(\rho) + \omega(\rho)}{b(\rho)} \right] \left( \pi_2 + \frac{\pi_2 - k \cdot \rho \cdot \pi_3}{\exp[\alpha(\rho) - \omega(\rho)] - 1} \right) \times \exp(-\Phi(\rho, 0)) \rho d\rho \quad (56)$$

$$N_B = \frac{2}{X_{AB}} \left( \frac{\varepsilon}{\tau} \right) CRT \int_0^1 \alpha(\rho) \rho d\rho \quad (57)$$

The solute concentration in permeate can be calculated by the equation [78-79]:

$$C_{A3} = C \left[ 1 + CRT \frac{l_1}{l_3} \right]^{-1} \quad (58)$$

Moreover, in work [80] the following equation for the rejection coefficient calculation was proposed:

$$R = 1 - \frac{\Phi K_c}{1 - (1 - \Phi K_c) \exp(-Pe)} \quad (59)$$

where Pe is the Peclet number.

In contrast with previous models, the surface force-pore flow model is complex and requires complex solution methods without visualization, the distinctive for the CFD methods. This determined the narrow range of this model application which was only used for the description of the ground waters purification from pesticides [80].

Also, in work [81] for the description of the pressure driven membrane processes including RO the Hagen-Poiseuille equation was considered:

$$u(r) = -\frac{1}{4\mu} \frac{dp}{dx} (R^2 - r^2) \quad (60)$$

However, this approach is more suitable for the simulation of the ultrafiltration and microfiltration.

Despite that, the models of this class take into account both diffusive and convective transport through the membrane, in work [82], the analytical solution-diffusion pore-flow model was presented. Also, in work [83] the similarity of the processes in the membrane with convective heat transfer was considered. However, that approaches were used rarely.

### 3.4 Computational fluid dynamics based models

As mentioned in work [1], the flow conditions have a significant influent on the operation of the processes during membrane separation, including mass transfer, concentration polarization, and fouling layers formation, the pressure drop in the membrane channels. Taking into account the critical importance of the hydrodynamic conditions not only for the membrane processes but for engineering in general, the development of the method for the mathematical description and analysis of the flow named computational fluid dynamics (CFD) is natural. The method itself is based on the mathematical description of the fluid flow, which includes the Navier-Stokes equation, the continuity equation, and the mass and energy conversation equation [84].

For the steady state laminar flow of the Newtonian fluid these equations can be written in a form:

- the continuity equation [84]:

$$\frac{\partial u}{\partial x} + \frac{\partial v}{\partial y} + \frac{\partial w}{\partial z} = 0 \quad (61)$$

- the Navier-Stokes equation [84]:

$$u \frac{\partial u}{\partial x} + v \frac{\partial u}{\partial x} + w \frac{\partial u}{\partial z} = -\frac{1}{\rho} \frac{\partial P}{\partial x} + \frac{\mu}{\rho} \left[ \frac{\partial^2 u}{\partial x^2} + \frac{\partial^2 u}{\partial y^2} + \frac{\partial^2 u}{\partial z^2} \right] \quad (62)$$

$$u \frac{\partial v}{\partial x} + v \frac{\partial v}{\partial x} + w \frac{\partial v}{\partial z} = -\frac{1}{\rho} \frac{\partial P}{\partial x} + \frac{\mu}{\rho} \left[ \frac{\partial^2 v}{\partial x^2} + \frac{\partial^2 v}{\partial y^2} + \frac{\partial^2 v}{\partial z^2} \right] \quad (63)$$

$$u \frac{\partial w}{\partial x} + v \frac{\partial w}{\partial x} + w \frac{\partial w}{\partial z} = -\frac{1}{\rho} \frac{\partial P}{\partial x} + \frac{\mu}{\rho} \left[ \frac{\partial^2 w}{\partial x^2} + \frac{\partial^2 w}{\partial y^2} + \frac{\partial^2 w}{\partial z^2} \right] \quad (64)$$

- mass conversation equation [84]:

$$u \frac{\partial C}{\partial x} + v \frac{\partial C}{\partial y} + w \frac{\partial C}{\partial z} = D \left[ \frac{\partial^2 C}{\partial x^2} + \frac{\partial^2 C}{\partial y^2} + \frac{\partial^2 C}{\partial z^2} \right] \quad (65)$$

In these equations:  $u$ ,  $v$ ,  $w$  are the velocity projections on the coordinate axes;  $P$  is the pressure;  $C$  is the solute concentration;  $\rho$  is the feed solution density;  $\mu$  is the feed solution viscosity;  $D$  is the diffusivity.

The equations are also represented in a similar way in works [85-97], including written for the two-dimension simplification [89, 91, 96], in the cylindrical coordinates [90], and matrix form [93]. Moreover, in works [93-94], the unsteady-state conditions were taken into account.

However, the equations (61) – (65) due to their awkwardness are often written in an operator form with using of the differential operators, including the full derivative operator, the Hamilton operator, the Laplace operator etc., and also the rules of the vector and tensor analysis. In this case, the equations of the mathematical model of the fluid flow can be written in a form:

- the Navier-Stokes equation [98]:

$$\rho(\bar{u} \cdot \nabla) \bar{u} + \nabla P - \mu \nabla^2 \bar{u} = 0 \quad (66)$$

- the continuity equation [98]:



$$\nabla \cdot \bar{u} = 0 \quad (67)$$

- mass conservation equation [98]:

$$D\nabla^2 C = \bar{u} \cdot \nabla C \quad (68)$$

The equations are written in a similar way, for example, in works [6, 99–126].

For accounting of the unsteady-state conditions these equations can be rewritten in a following way [127]:

$$\frac{\partial \rho}{\partial t} + \nabla \cdot (\rho u) = 0 \quad (69)$$

$$\frac{\partial(\rho u)}{\partial t} + (u \cdot \nabla) \rho u = -\nabla p + \nabla \cdot (\mu \nabla u) \quad (70)$$

$$\frac{\partial C}{\partial t} + (u \cdot \nabla) C = \nabla \cdot (D \nabla C) \quad (71)$$

The similar equations are in works [128-129].

Also, the equations are represented in the reviews [6-8].

As it was mentioned above, equations (60)-(64) are suitable for the laminar flow. However, in the channels of the membrane apparatuses, there exist favorable conditions for turbulence development. Therefore, the models of flow are often supplemented by turbulence models. The k- $\omega$  and k- $\varepsilon$  models are most widely used. The distribution between them is represented in Figure 7.

The k- $\varepsilon$  turbulence model operate by the terms of the specific turbulent kinetic energy k and the dissipation rate  $\varepsilon$ . The equations of this model are following [138]:

$$\frac{\partial(\rho k)}{\partial t} + \nabla \rho \bar{u} k = \nabla \cdot \left[ \left( \mu_k + \frac{\mu_{eff}}{\sigma_k} \right) \nabla k \right] + \mu_{eff} S^2 - \rho \varepsilon \quad (72)$$

$$\begin{aligned} \frac{\partial(\rho \varepsilon)}{\partial t} + \nabla \rho \bar{u} \varepsilon = & \nabla \cdot \left[ \left( \mu_k + \frac{\mu_{eff}}{\sigma_k} \right) \nabla \varepsilon \right] + \\ & + C_1 S \rho \varepsilon - C_2 \frac{\rho \varepsilon^2}{k + \sqrt{v \varepsilon}} \end{aligned} \quad (73)$$

The physical meanings of the parameters in equations (72) and (73) are described in work [138].

This model was also used, for example, in works [91, 137, 139].

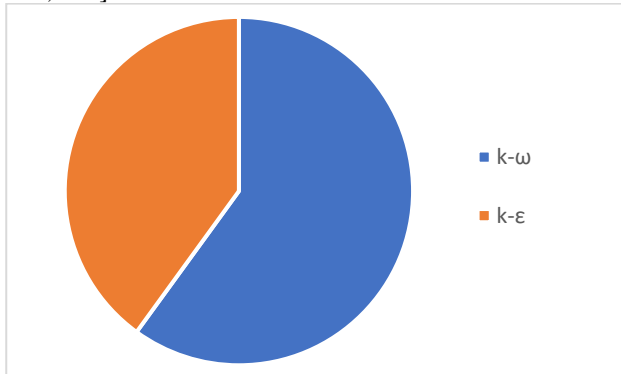


Figure 7 – The distributions of the main turbulence models in the chosen articles

In contrast, the other model uses the value of the specific dissipation rate  $\omega$  instead of  $\varepsilon$ . This model can be represented in a form [97]:

$$u_j \frac{\partial u_i}{\partial x_j} = -\frac{1}{\rho} \frac{\partial P}{\partial x_i} + \frac{1}{\rho} \frac{\partial}{\partial x_j} \left( (\mu + \mu_t) \frac{\partial u_i}{\partial x_j} \right) \quad (74)$$

where the turbulent viscosity can be calculated by following equation [97]:

$$\mu_t = \rho \frac{a_1 k}{\max(a_1 \omega; \Omega F_2)} \quad (75)$$

The equations for calculations of the k and  $\omega$  values according this model are following [97]:

$$u_j \frac{\partial(\rho k)}{\partial x_j} = \tau_{ij} - \beta^* \rho \omega k + \frac{\partial}{\partial x_j} \left[ (\mu + \sigma_k \mu_t) \frac{\partial k}{\partial x_j} \right] \quad (76)$$

$$\begin{aligned} u_j \frac{\partial(\rho k)}{\partial x_j} = & \frac{\gamma}{v_t} \tau_{ij} \frac{\partial u_i}{\partial x_j} - \beta \rho \omega^2 + \frac{\partial}{\partial x_j} \left[ (\mu + \sigma_\omega \mu_t) \frac{\partial \omega}{\partial x_j} \right] + \\ & + 2\rho(1 - F_1) \sigma_{\omega 2} \frac{1}{\omega} \frac{\partial k}{\partial x_j} \frac{\partial \omega}{\partial x_j} \end{aligned} \quad (77)$$

This model was also used, for example, in works [85-88, 97, 126].

Since the equations of models are differential, the starting and boundary conditions are needed for the obtain the result. These conditions strongly depend from the geometrical and physical conditions of the considered process, for example, for the equations (61) – (65) for the case of the fluid flow in the spiral wound membrane channel with the spacer in work [84] the following boundary conditions were applied:

- inlet boundary conditions:

$$C = C_0; u = \frac{m}{\rho A_i}; v = w = 0 \quad (78)$$

- membrane boundary conditions:

$$C = C_m; u = v = w = 0 \quad (79)$$

- filament boundary conditions:

$$\frac{\partial C}{\partial n} = 0; u = v = w = 0 \quad (80)$$

- symmetry face boundary conditions:

$$\frac{\partial C}{\partial z} = 0; \frac{\partial u}{\partial z} = \frac{\partial v}{\partial z} = \frac{\partial w}{\partial z} = 0 \quad (81)$$

- outlet boundary condition:

$$P = P_0 \quad (82)$$

Also, the boundary conditions are described in details, for example, in works 89-90, 92, 109, 117, 127-132, 134, 140], and also in the review work [8].

Due to the complexity of the equations described above, the mathematical models should be solved by numerical methods, mainly by using specialized software. In work [1], it was noticed, that for the case of RO, the most widely used commercial software included ANSYS FLUENT and ANSYS CFX, however, in the considered period, the range of applied software was wider. The distribution of them in chosen publications is shown in figure 8. Since the ANSYS software is still the most widely used, it is reasonable to consider the ratio between the main algorithms (FLUENT and CFX) that are shown in figure 9. Thus, the ANSYS FLUENT was most widely used, in particular, in works [90-91, 95-96, 107, 110, 116, 118, 124, 126-127, 133, 137-139, 141-145]. The ANSYS CFX was applied to a lesser extent, for example in works [85-88, 93, 113, 128-131, 134, 146-147, 121]. Moreover, the ANSYS was used without pointing out the algorithm in works [84, 99, 121, 123]. Among the other software un should be noticed the wide range of applications of COMSOL Multiphysics, for example, in works [98-99, 101-106, 111-112, 119, 122-123, 148], and open-source product OpenFOAM [92, 94, 114, 132, 135, 137].

The other software, including MATLAB [102, 104, 117], ROSA [149-151], NUMECA [152], MUSUBI [153], was used rarely. Also, in work [154], it was carried out the analysis of the possibility of applying the RO seawater desalination by the commercial systems CORMIX, VISUAL PLUMES, and VISJET. Meanwhile, the popular engineering system SolidWorks was not used almost. Only in work [121], the geometry was created in this system, whereas the calculations were carried out in ANSYS.

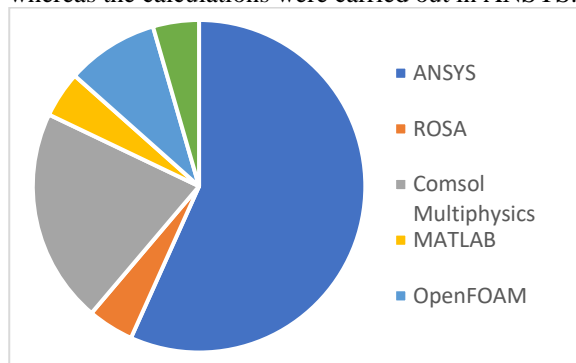


Figure 8 – The application of the software for the RO simulations

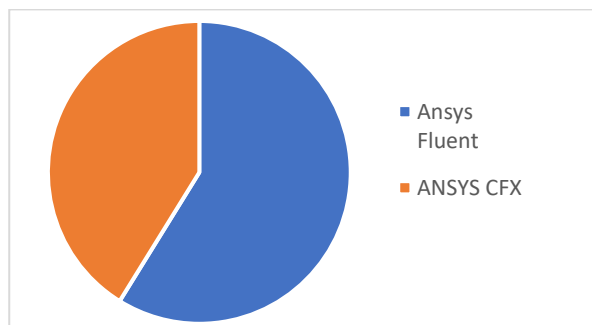


Figure 9 – The application of the algorithms of the ANSYS software for RO simulation

In some works, namely [23, 89, 97, 100, 108-109, 140, 155-157], it was not pointed out the applied software or mentioned that the algorithm of the mathematical model solution was designed independently.

Taking into account the importance of the geometry of the channels for the simulation by the CFD method, great attention was dedicated to the module design. As in others approaches, the greatest number of researches were carried out for the spiral wound membrane modules, in particular in works [6, 23, 84, 88, 98, 101, 104, 106, 110, 112-114, 117, 121, 141, 149, 151, 155-157]. In this case, it should be noticed, that in work [149] it was declared that the influence of the channel curvature is significant and the neglect of this factor can lead to a significant mistake. At the same time, the channels of the spiral wound membrane modules were conditionally rolled out into the plane, in particular in works [6, 88-89, 104]. Also, in a significant number of works the hollow fiber modules were considered [86, 106, 116, 121, 125-126, 137, 139], whereas the plate and frame modules were considered in a lesser number of the researches [91, 108-109]. The same situation is observed for the tubular modules [127, 137], and also for the multichannel ceramic modules [124] and similar designs [152]. Also, in some works the original designs were considered including rotating [90, 142] and test and lab cells [98, 135, 143]. The works, in which the patterned [111] and corrugated [97] membrane surface, should be noticed individually.

Taking into account the importance of the spiral wound modules and the correspondingly large number of studies, it was expected, that a large number of the investigations by CFD methods were dedicated to the influence of spacers on the process performance. Thus, in work [147], the important parameters, which impact the process, were pointed out. They include the angle between the spacer filament, the spacer thickness, and the filament placement in the channel. In some works, for example [92, 141, 144, 155] the commercial spacers designs were considered. Also, it should be noticed, that in works [87, 92, 95] the spacer filament was considered cylindrical, and in work [144] it was considered with the elliptical cross-section. Therefore, along with this, it should be pointed out the works [104] and [105], in which the real geometry of the spacer was determined by the microscope measurements and X-ray computer tomography and reproduced in the CFD programs. Moreover, in the result of the comparison with the ideal geometry, in work [104] it was mentioned, that the cylindrical form of the spacer filament is a good approximation, whereas in work [105] it was pointed out the possible inaccuracies (in particular the overestimation of the pressure drop), which can be obtained without taking into account the real geometry of spacer filament. The comparison of the wound and non-wound spacers was another direction of the investigations, as was shown in works [84, 103, 153]. In this case, in work [103], it was pointed out, that the wound geometry has advantages, while in work [153] it was shown the bigger pressure drop in the channel with the wound spacers. Great attention was dedicated to the spacer filament placement by the channel width, in particular in works [96, 100, 114, 119, 129, 134].

At that, in most cases, it was pointed out, that the best results were obtained for the zigzag placement of the filament. The influence of the angle between spacers was investigated in works [87-88, 106, 145, 155-157]. In work [1] it was pointed out, that the determination of the optimal angles is still debatable. The result of the consideration of the mentioned publication confirms this statement. In contrast with the previous period, in 2011-2020, it was proposed a large number of novel spacer designs, in particular in many studies the design with the different thicknesses of the filament between the spacer nodes, in particular in works [99, 101, 102, 112, 113, 118]. Also, it was proposed the sinusoidal spacer design [123] and the design with the screw thread on the filament [107]. Despite the benefits of the proposed designs, there are some doubts about the possibility of realizing these geometrical forms for the manufacturing of the real spacers taking into account their real thickness. The same doubts are also related to the original design of the hollow fibers with the specific cross-section, with was described in the work [116]. These doubts are appearing from the accounting of the results of the comparison of the real and ideal geometry, carried out in works [104-105]. Moreover, in work [148] it was also pointed out the significant influence of the deviations from ideal geometry for the multibore polymer membrane modules. It also should be noticed the application of the multilayer spacers [121, 130]. The novel designs of the spacers were also considered in the review [8].

In works using the CFD method, the separation process for which the simulation is carried out is not often pointed out, however, in most cases, this is about the desalination processes [85-87, 101, 108-109, 152].

In general, the mathematical simulation of the RO using CFD methods, as was predicted in work [1], is intensively developing and, likely, in the near future, will remain the most effective and widely used.

### 3.5 Artificial neural networks based models

In work [1], among the novel approaches except the CFD methods, the artificial neuron networks (ANN) were considered. Such systems are built by analogy with the architecture of the biological nervous systems, which mainly consist of simple nerve cells or neurons, which work in parallel for the simplification of quick decisions. Similarly, the neuron networks are made from a large number of primitive processing elements, which are organized in a massive parallel set. Then, in the neuron networks the artificial connections (synapses), connect these elements. They are characterized by the set of the weight coefficients, which could be updated in the learning process [79, 158-160]. Thus, the artificial neuron networks are the computational method for comparing the input and output data from the process by the nonlinear regression model. The ANN method has the ability to analyze the relationship between input and output data based on the functions of the biological neuron networks, as mentioned above. The simple architecture of the ANN includes three-layer namely, input, hidden, and output. The input signal received from an external source is multiplied by the

mentioned above weight coefficients. When the result of the multiplication exceeds the threshold, the signal would be released and sent to the output depending on the ANN activation function. In this respect, three stages, namely training, testing, and validating, with several computational operations are applied to achieve the desired goal through ANN [161].

The advantages of the simulations using the ANN include [160]: (1) the ability of the simulation of complex relationships, which is impossible for the models based on conventional mathematical methods; (2) in many cases the ANN has higher accuracy than conventional mathematical models; (3) the ANN can be adapted with new data and modernized with them; (4) the best combination of the design parameters in the ANN can be obtained by the trial and error method.

In each stage of the ANN, the main computational operation has the following form [161]:

The equations of the output signal for any hidden or output layer are determined by the following equations [161]:

$$a_1 = \sum_{i=1}^{i=n} (W_i X_i + b1) \quad (83)$$

$$a_2 = \sum_{j=1}^{j=k} (W_j a_1 + b2) \quad (84)$$

where  $a_1, a_2$  are the output signals of the first and second layer correspondingly;  $X$  is input parameter;  $W$  and  $b$  are the weight coefficients and bias, correspondingly [161].

The activation function is used for the data normalization in range  $[0 -1]$  and  $[-1 1]$ , which is discrete or continuous in a form of sigmoid [161]:

$$f(s) = \frac{1}{1 + e^{-s}} \quad (85)$$

or in a form of the hyperbolic tangent:

$$f(s) = (e^s - e^{-s}) / (e^s + e^{-s}) \quad (86)$$

$s$  is the value of the input parameter. The network may be linear or nonlinear in the activation function [161]:

$$f = \begin{cases} 1 & \text{if } s > 0 \\ -1 & \text{otherwise} \end{cases} \quad (87)$$

The normalization equation has following form [161]:

$$s_i = \frac{0.8}{d_{\max} - d_{\min}} (d_i - d_{\min}) + 0.1 \quad (88)$$

$d_{\min}, d_{\max}$  and  $d_i$  are minimum, maximum and  $i$  value of the input/output data correspondingly. The predicted or target equation can be represented in a form [161]:

$$Y = \sum_{j=1}^{j=k} f_2 \left( W_j f_1 \left( \sum_{i=1}^{i=n} W_i X_i \right) \right) \quad (89)$$

$Y$  is predicted output value. The weight matrices are calculated by applying an error back-propagation method.

The accuracy of the weight coefficient depends on the minimal error ( $E$ ) of the output  $\{z(k); 1 \leq k \leq K\}$  on the learning stage and calculated using the sum of the square error [161]:

$$E = \sum_{k=1}^K [e(k)]^2 = \sum_{k=1}^K [d(k) - z(k)]^2 = \sum_{k=1}^K [d(k) - f(W_x(k))]^2 \quad (90)$$

where  $[W_x]$  is the weight matrices;  $[x]$  is input vector; and  $d$  is desired target value.

In general, there are three criteria used for the evaluation of the ANN performance, namely coefficient of correlation ( $r$ ), mean square error, and mean absolute error [162].

The ANN are especially effective when it is difficult to develop mechanistic models [161].

In some works, the ANN were used together with other methods, in particular with the solution-diffusion model [158, 163], the surface force-pore flow model [79], the CFD methods [164], and also with the surface response methodology [166]. Moreover, in work [79], it was noticed, that the ANN predictions were more accurate than the surface force-pore flow model ones. Also. The ANN were applied for consideration of the systems with a high level of fouling [167-168], moreover, in work [168], it was mentioned that mechanistic models oversimplify the fouling phenomena.

In most cases, the ANN methods of simulation were used for the analysis of the desalination processes [158, 160, 162, 166, 168-169] and the water and wastewater treatment [161, 163, 165, 167].

In general, during 2011-2020, ANN were used for the RO process simulation in a limited range. The likely reason for this is the high enough level of the development of mechanistic models, in particular, the suitability of the CFD methods for these purposes. The ANN can be used the most effectively in systems with a high level of fouling [167-168] or systems with nonconventional energy sources [163, 169].

### 3.6 Molecular dynamics based models

In addition to the CFD and ANN methods, the molecular dynamics (MD) methods are a relatively new approach to the RO process. As in the case of CFD, this method is based on the numerical solution of the Newton equations of motion, but on the molecular level [10].

The concept of classical molecular dynamics is based on Newtonian mechanics. According to the second Newton law, the relationship among the mass, acceleration, and force exerted to the particle  $i$  is described by the equations [10]:

$$F_i = m_i a_i = m_i \frac{d^2 r_i}{dt^2} \quad (91)$$

where  $m_i$  is the particle mass;  $a_i$  is the acceleration;  $F_i$  is the force exerted to the particle;  $r_i$  is the distance between particles;  $t$  is the time.

The Newtonian force also can be expressed in a form of the gradient of the potential energy [10]:

$$F_i = -\nabla_i U(r_i) = -\frac{\partial U(r^N)}{\partial r_i} \quad (92)$$

Using the relationships, represented by equations (90) and (91), it is possible to obtain the trajectories for all atoms, which are described by the successive positions, velocities, and momenta. These trajectories become the initial data for the prediction of the bulk properties of the systems, with further connections to the physical phenomena [10].

Inside the determined system, the pair of atoms are in interaction, irrespective of that they are bounded or separated by the distance. These interactions formed the basis of the simulation by the MD method. From this force, the equation for the potential energy can be obtained for the description of the stretching, vibrations, and rotation of the particles around the bounds as a result of the intermolecular force. This equation can be represented in the following way [10]:

$$U_{total} = U_{bond} + U_{angle} + U_{dihedral} + U_{vdW} + U_{Coulomb} + U_{external} \quad (93)$$

The values  $U_{bond}$ ,  $U_{angle}$  and  $U_{dihedral}$  take into account the stretching, bending, and torsion, which take place in atoms, correspondingly. On the other hand, the values  $U_{vdW}$  and  $U_{Coulomb}$  describe the non-bounded interactions. Moreover, the van der Waal's forces have origin in the weak force existing for the non-bounded atoms, whereas the  $U_{Coulomb}$  is used for the description of the electrostatic interactions, which are caused by electrostatic interactions. The last term of the total potential energy  $U_{external}$  takes into account the external forces, applied to the system. In the investigation of the RO process, the main external force is the applied pressure [10].

The potential energy of the intermolecular interaction also can be described by the following equation [171, 172]:

$$U_{(r_{ij})} = 4\epsilon_{ij} \left[ \left( \frac{\sigma_{ij}}{r_{ij}} \right)^{12} - \left( \frac{\sigma_{ij}}{r_{ij}} \right)^6 \right] + \frac{q_i \cdot q_j}{4\pi\epsilon_0 r_{ij}} \quad (94)$$

where  $r_{ij}$  is the distance between particles  $i$  and  $j$ ;  $q_i$  and  $q_j$  are the partial charges of the  $i$  and  $j$ ;  $\epsilon_{ij}$  and  $\sigma_{ij}$  are empirical Lennard-Jones parameters.

The MD method has an advantage, which consists of the ability to achieve the temporal and spatial solutions which are difficultly available by experimental investigations. For example, the solutions are possible for the dimension less than Angstrom and the periods of time less than a femtosecond [173].

Taking into account that the considered approach requires large volumes of calculations, the necessity of the

special software application is evident. For the MD methods realization of the many software packages, algorithms, and codes. In particular, for the RO simulations the following software was used: Visual Molecular Dynamics (VMD) [171-172, 174-178], Nanoscale Molecular Dynamics (NAMD) [171-172, 174-175, 179-180], Groningen Molecular Simulation package (GROMACS) [176-178, 181-183], Chemistry at Harvard Molecular Mechanics (CHARMM) [172, 175-176, 184], Large-scale Atomic/Molecular Massively Parallel Simulator (LAMMPS) [185-187], Materials Studio [181, 188-191], especially Amorphous Cell package of Material Studio software [192-193], Assisted Model Building and Energy Refinement (AMBER) [180, 192-195], Optimized Potential for Liquid Simulations (OPLS-AA) [181-182], Condensed-phased-optimized Molecular Potential for Atomistic Simulation Studies (COMPASS) [188, 190], DL\_POLY [194-195]. The data about such software developers and more detailed pieces of information about its application are represented in the review work [11].

During the simulation by MD methods, statistical techniques were used, including the Monte-Carlo method [174, 192-194] and surface response methodology [189]. A more detailed description of the MD methods is represented in the review work [10].

Taking into account the features of the method, during its application special attention was dedicated to the membrane material. In many works, conventional materials, such as polyamides [11, 175, 179, 184, 187, 190, 192-195], sulfonated diamine [189], and polyether sulphones [181], were considered. At the same time, a significant number of publications were dedicated to the use of membrane manufacturing such novel materials as graphene [9, 182, 187, 196] and graphene oxide [178, 197]. Also, the considered method was used for the analysis of the performance of the membrane made using the carbon [172, 176, 196, 198] and aluminosilicate [185], nanoporous carbon [199], boron nitride [171, 200], fullerite [188], and MoSe<sub>2</sub> [177]. It should be noticed that in work [188] it was claimed that the fullerite membranes have the higher flux than the graphene and conventional membranes, and in work [177], it was declared that the flux of the productivity of the proposed membranes is who orders of magnitude higher than the commercially available membrane one.

In most cases, the investigation was dedicated the water treatment [175-176, 180, 190-191, 194-195, 199, 201], including desalination [11, 177, 182-185, 187-188, 192-193, 196-197, 200] and the heavy metal ions removal [171-172, 178].

### 3.7 Optimization and process control

In work [1], it was noticed that the determination of the optimal condition and processes control are the important practical application of the mathematical simulation of the pressure driven membrane processes, including RO. The large number of publications dedicated to these questions in the period from 2011 to 2020 completely confirm this statement.

Also, in work [1] it was noticed, that the optimization problem consists in finding the most beneficial values of the operation parameters. The important factor of the successive optimization procedure includes the choice of the target function and the optimization criterion. As in 2020-2010, in the considered period in most works authors used the economical optimization criteria, primarily the minimization of costs [49, 61, 74-75, 202-217], and also the minimization of the energy consumption, which is the significant part of the operational cost [27, 38, 49, 66, 73, 204-205, 219-228]. Also, the economic criteria included the profit maximization [229-230], and the minimization of the cost factor, which in work [231] was determined as the ratio of the water price and energy price in a hybrid system with reverse osmosis and pressure retarded osmosis. The main technological parameters for optimization included maximization of the removal of the component from solution 27, 36, 38, 63, 200, 221, 232-233], minimization of the concentration [234], maximizing of the permeate concentration [35], maximizing of the recovery ratio [235], maximizing of the productivity [236-237], and minimization of the applied pressure [36]. The other direction of the optimization involved the minimization of the fouling level [238] and the minimization of the environmental impact [230]. In the set of works, multiobjective optimization was applied [239-240].

In many works, the optimization was carried out based on the conventional mathematical models described in previous chapters. In particular, the solution-diffusion model was the most widely used [35-36, 38, 61, 66, 75, 204, 209, 214, 218, 221, 241]. Also, it was applied the Kedem-Katchalsky model [205, 219], Spiegler-Kedem model [27], Kimura-Surirajan [73], the surface force-pore flow model [78], and also the molecular dynamics models [200]. Moreover, the factor experiment method and other regression and statistical methods were applied [212, 228, 232, 235, 243-244]. The questions of the optimal control and processes control were considered in the works [220, 236-237, 245-248].

For the optimization problem solution, a large number of methods and algorithms can be used. In the considered researches the most widely used methods included the nonlinear programming [35, 49, 61, 74-75, 204-211, 218, 222, 229-230], the generic algorithm [28, 38, 237, 241-242], the particle swarm method [202, 247, 250], the sequential quadratic programming [219, 233], the surface response methodology [232], the pattern search algorithm [251], the harmony search algorithm [66], and the bees algorithm [213]. The work [216] should be pointed out, since in it the nineteen optimization algorithms were considered and compared.

For the solution of the considered optimization problems the wide range of the software and programming languages was applied including Matlab [73, 203, 250, 252], gPROMS [63, 218, 235], GAMS [49, 209, 211, 246, 254], Design-Expert [232], ASPEN [214], ChemCAD [215], ROSA [206-207], Modelica [219], C++ [36, 38], R [244].

As in the most considered RO simulation methods, the optimization was applied mainly for the analysis of the water treatment processes, primarily the seawater and brackish water desalination [49, 61, 66, 73-75, 200, 202-203, 206-210, 212-217, 219-227, 229, 234-235, 237-240, 242, 244-246, 248-250, 251-255], the potable water production from ground waters [256-257], the wastewater treatment [230-231, 238, 258], and recycling [211], and also the ultrapure water production [259]. In some works, it was considered the special pollutant removal including chlorophenol [36, 204, 233, 243], N-nitrosamine [27, 63], arsenic [205], boron [218] and bentazon [232]. Except for the water treatment, the concentration of the apple juice [35] and the maple syrup [228] was also considered.

The optimization methods appear to be effective for the analysis of the hybrid systems performance, in which the RO was combined with thermal distillation [214-215, 241], forward osmosis [238], pressure retarded osmosis [219, 229, 231], and forward osmosis and electrodialysis [224]. The other important direction was the optimization of the system with renewable energy sources [216, 260], including solar [202, 216, 253] and wind [216] energy.

It should be noticed, that the application of the optimization methods can give a significant economic effect, for example, it was noticed the achievement of decreasing of energy consumption by 16% in work [227], the decreasing operational cost by 26% in work [209], and the economy of the 27 % of the annual costs of the obtained product in work [211].

### 3.8 Energy analysis

It was mentioned above that energy consumption is a significant part of the operative costs during RO exploration. In the period from 2010 to 2020, a large number of articles dedicated to calculations and analysis of the energy parameters of RO were published, therefore, it is reasonable to consider this direction in general terms.

Mainly, the energy analysis of the RO systems was based on the mass and energy balances [43, 228, 261-266], theoretical calculations of the specific energy consumption [43, 228, 261-266], the exergy analysis [15, 43, 241-242, 263, 265, 275, 286-290], the pinch-analysis [292], and the calculations of the thermodynamical effectivity [293-294].

It should be noticed that, in many cases, the energy and exergy balances were written for the full set-up rather than RO apparatuses. At that the RO can be combined with energy recovery systems (including pressure exchangers and turbines) [276, 288-289, 290], Rankin cycle [296], internal combustion engine [269], electrodialysis [268, 270], distillation [262-263, 282, 290-291], humidification-dehumidification [43], membrane distillation [278, 298], forward and pressure retarded osmosis [278, 299], photovoltage system [264], and capacitive deionization [284].

As in the case of the optimization, the grate attention was dedicated to renewable energy sources including solar energy [262-264, 272-273, 275, 289, 293, 297, 301-303], wind energy [267, 287, 262-263, 301-302, 304], and also tidal energy [266, 272].

As in all previous cases, the high effectiveness of the analysis was achieved via the application of specialized software and programming languages. For the energy analysis such means as ROSA [150, 265, 272, 295, 300], Matlab [261, 295], ASPEN [205], Visual Design Software [288], WAVE [305], EES [289], and R [244] were widely used.

In most cases, the desalination processes were considered. Also, in many works, the significant economical effect was pointed out. For example, in work [287] on the results of the exergo-economic analysis, the authors managed to find a way of decreasing energy consumption by 24%. In works [288] a similar analysis shows that the application of the turbine allows to decrease the energy consumption by 49%, and the application of the pressure exchanger – by 77. In work [289]. It was shown that application of the Pelton turbine allows for recovery of 24% of the consumed energy.

### 3.9 Economic analysis

During consideration of most approaches, especially optimization and energy analysis, it was pointed out that the economic parameters have significant importance for the performance analysis of the RO systems. Therefore, it is reasonable also to consider in general terms the economic methods of the analysis of the considered process.

Except optimization [202, 204-205, 231, 241] and energoeconomic analysis [205, 230, 241, 266-270, 280, 285-287, 306], the economical models included the determination of the relationship for calculation of the capital cost (CAPEX) [55, 204-205, 234, 230, 266, 268, 270, 280, 286, 297, 300, 307-317], operating costs (OPEX) [55, 204-205, 209, 230, 234, 266, 280, 300, 307, 309-318], and product price [268, 274, 280, 297-298, 302, 306-307, 314, 319-324]. Among other parameters the profit [325], cost saving coefficient [319], cost factor [231], and water price index [326] can be pointed out. In certain works, the simplified economic balance [327] and socio-economic evaluation [328] were considered.

The other joint characteristic of the investigation based on economic analysis with ones based on optimization and energy analysis is the significant number of works dedicated to hybrid systems and systems with renewable energy sources. In particular, the hybrid systems RO-distillation were considered in works [55, 230, 241, 307-308, 314-315], and the works [321, 241, 300, 309, 311] were dedicated to the systems RO-FO and RO-PRO. The other hybrid systems including electrodialysis [270, 310], crystallization [268, 270], and power plant [55, 274]. Among the alternative energy sources, the most attention was dedicated to solar energy [202, 297, 302, 308, 320-321, 328]. Wind energy [302, 306], tidal energy [266], and geothermal energy [314] were also considered.

Among the software, in works dedicated to the economic analysis of the RO systems, it was mentioned ROSA [231, 266, 324], COMFAR III [323], and ESS [324].

As in all other approaches to the RO simulation, in most cases, the application of RO for the seawater and brackish

waters desalination [55, 202, 209, 234, 241, 266-270, 274, 280, 287, 297, 302, 306-309, 311-312, 314, 317-324] was considered. In addition, the questions about wastewater treatment [298, 300, 310, 315-316, 327], including the removal of certain pollutants such as chlorophenol [204] and arsenic [205], were regarded.

#### 4 Discussion

In certain works, the other approaches, which cannot be related to the described above groups, were applied. Those models can be based on the empirical data (both with and without combination with conventional models) [329-336], the mass and energy balances [337-341], the Monte-Carlo method [342-344], the concentration polarization models [345-347] and osmotic pressure [348], the boundary layer theory [349], the dynamic modeling [350], the materials flow analysis [351], the risk and fault analysis [352-353], the numerical methods [354], the chemical kinetics and equilibrium [355], or its combinations [356]. However, such investigations were low numerous and it does not seem possible to define some of them as perspectives.

It should also be noted, that in some works for the RO description the extended Nernst-Planck equation [358-359] and the Donnan equilibrium [359] were used, however, such approaches are conventionally used for the NF, as was shown in work [1]. Moreover, the special software (such as ROSA or Q+), which was widely used for the analysis of the economical and energy parameters of RO systems, can be also used for the simulation of the technological parameters and system design, as it was realized, for example, in works [340, 360-365].

#### 5 Conclusions

The technological, energetic, and economic advantages of the reverse osmosis process in conjunction with the benefits of the mathematical simulation determined the considerable spread of this type of investigation. Therefore, it is natural, that the stable trend increasing in the number of publications dedicated to the reverse osmosis simulation is observed. The analysis of publications about this question in the period from 2011 to 2020 allows also traces the main direction and the advantages and disadvantages of the main approaches to the RO simulations.

Thus, the number of publications dedicated to the application of the CFD methods for the mathematical simulation of RO appears to be the largest. The increasing computational power of computer equipment and the development of specialized software, including the appearance the open-source programs, are the evident

reasons for this. It is logical to assume, that the same factors promoted the significant increase in the application of the molecular dynamics methods in comparison with the previous decade. Such a trend allows us to conclude, that these two approaches will remain the most widely used in the near future. The main advantages of this method consist in the possibility to obtain a deep understanding of the processes which take place in the membrane apparatus (CFD) or in the membrane itself and on its surface (MD). They also allow us to determine the influence of the large number of factors affecting the process and, therefore, the productivity and effectiveness of separation. However, the simulation using these methods requires the application of more complex and cumbersome calculation methods, and also a high level of skills of operation in corresponding software.

On the other hand, the published results indicate that the interest of the researchers and engineers in hybrid systems, in which the RO is combined with other processes, mostly with distillation, forward osmosis, and renewable energy sources increased significantly. For the simulations of such systems, it is reasonable to apply the simulation techniques which require simpler calculation methods. It was quite unexpected that, for these purposes, the solution-diffusion model was used in the widest range. In the considered period it was used both for the direct RO simulation and for the optimization, energy and economic analysis, and even as boundary conditions in CFD investigation.

At the same time, the application of the irreversible thermodynamics methods, pore flow based models, and other diffusion based models was limited and, likely, further these models will be used mainly for the specific processes analysis. Also, the application of artificial neuron networks was limited, which probably is due to the fact that the possibility of the mechanistic model construction is relatively high for the case of RO. In these conditions, the ANN will be the most effective in systems that are significantly complicated by concentration polarization and fouling.

Therefore, based on the current review it is possible to choose the strategy for the simulation of the RO system. It also should be noticed that represented in the current review the analysis of the software applied for the reverse osmosis simulation, would be useful for educational purposes.

#### 6 Acknowledgments

Authors would like to thank the Armed Forces of Ukraine, National Guard, Territorial Defense, Volunteers for providing security to perform this work. This work has become possible only because resilience and courage of the Ukrainian Army.

## References

1. Huliienko S. V., Korniienko Y. M., Gatilov K. O. (2020). Modern trends in the mathematical simulation of pressure-driven membrane processes. *Journal of Engineering Sciences*, Vol. 7(1), pp. F1–F21, doi: [https://doi.org/10.21272/jes.2020.7\(1\).fl](https://doi.org/10.21272/jes.2020.7(1).fl)
2. Jarzyńska M., Pietruszka M. (2011). The application of the Kedem–Katchalsky equations to membrane transport of ethyl alcohol and glucose. *Desalination*. Vol. 280, Issues 1–3, pp. 14–19, doi: <https://doi.org/10.1016/j.desal.2011.07.034>
3. Al-Obaidi M.A., Kara-Zaitri C., Mujtaba M. (2017). Scope and limitations of the irreversible thermodynamics and the solution diffusion models for the separation of binary and multi-component systems in reverse osmosis process. *Computers & Chemical Engineering*. Vol. 100, pp. 48–79, doi: <https://doi.org/10.1016/j.compchemeng.2017.02.001>
4. Qasim M., Badrelzaman M., Darwish N.N., Darwish N. A., Hilal N. (2019). Reverse osmosis desalination: A state-of-the-art review. *Desalination*. Volume 459, pp. 59–104, doi: <https://doi.org/10.1016/j.desal.2019.02.008>
5. Ahmed F. E., Hashaikeh R., Diabat A., Hilal N. (2019). Mathematical and optimization modelling in desalination: State-of-the-art and future direction. *Desalination*. Vol. 469, 114092, doi: <https://doi.org/10.1016/j.desal.2019.114092>
6. Karabelas A.J., Kostoglou M., Koutsou C.P. (2015). Modeling of spiral wound membrane desalination modules and plants – review and research priorities. *Desalination*. Vol. 356, pp. 165–186, doi: <https://doi.org/10.1016/j.desal.2014.10.002>
7. Keir, G., Jegatheesan, V. (2014). A review of computational fluid dynamics applications in pressure-driven membrane filtration. *Reviews in Environmental Science and Bio/Technology*. Vol. 13, pp. 183–201, doi: <https://doi.org/10.1007/s11157-013-9327-x>
8. Toh K. Y., Liang Y. Y., Lau W. J., Fimbres Weihs G. A. (2020). A Review of CFD Modelling and Performance Metrics for Osmotic Membrane Processes. *Membranes*. Vol. 10, Is. 10, 285, doi: <https://doi.org/10.3390/membranes10100285>
9. Cohen-Tanugi D., Grossman J. C. (2015). Nanoporous graphene as a reverse osmosis membrane: Recent insights from theory and simulation. *Desalination*. Vol. 366, pp. 59–70, doi: <https://doi.org/10.1016/j.desal.2014.12.046>
10. Ebro H., Kim Y. M., Kim J. H. (2013). Molecular dynamics simulations in membrane-based water treatment processes: A systematic overview. *Journal of Membrane Science*. Vol. 438, pp. 112–125, doi: <https://doi.org/10.1016/j.memsci.2013.03.027>
11. Ridgway H. F., Orbell J., Gray S. (2017). Molecular simulations of polyamide membrane materials used in desalination and water reuse applications: Recent developments and future prospects. *Journal of Membrane Science*. Vol. 524, pp. 436–448, doi: <https://doi.org/10.1016/j.memsci.2016.11.061>
12. Wang J., Dlamini D. S., Mishra A. K., Pendergast M. T. M., Wong M. C.Y., Mamba B. B., Freger V., Verliefdé A. R.D., Hoek E. M.V. (2014). A critical review of transport through osmotic membranes. *Journal of Membrane Science*. Vol. 454, pp. 516–537, doi: <https://doi.org/10.1016/j.memsci.2013.12.034>
13. Ismail A. F., Matsuura T. (2018). Progress in transport theory and characterization method of Reverse Osmosis (RO) membrane in past fifty years. *Desalination*. Vol. 434, pp. 2–11, doi: <https://doi.org/10.1016/j.desal.2017.09.028>
14. Alsarayreh A. A., Al-Obaidi M. A., Patel R., Mujtaba I. M. (2020). Scope and Limitations of Modelling, Simulation, and Optimisation of a Spiral Wound Reverse Osmosis Process-Based Water Desalination. *Processes*. Vol. 8, Is. 5, 573, doi: <https://doi.org/10.3390/pr8050573>
15. Park K. Kim J., Yang D. R., Hong S. (2020). Towards a low-energy seawater reverse osmosis desalination plant: A review and theoretical analysis for future directions. *Journal of Membrane Science*. Vol. 595, 117607, doi: <https://doi.org/10.1016/j.memsci.2019.117607>
16. Abejón R., Garea A., Irabien A. (2012). Analysis, modelling and simulation of hydrogen peroxide ultrapurification by multistage reverse osmosis. *Chemical Engineering Research and Design*. Vol. 90, Is.3, pp. 442–452, doi: <https://doi.org/10.1016/j.cherd.2011.07.025>
17. Abejón R., Garea A., Irabien A. (2012). Integrated countercurrent reverse osmosis cascades for hydrogen peroxide ultrapurification, *Computers & Chemical Engineering*, Vol. 41, pp. 67–76, doi: <https://doi.org/10.1016/j.compchemeng.2012.02.017>
18. Fujioka T., Khan S. J., McDonald J. A., Roux A., Poussade Y., Drewes J. E., Nghiem L. D. (2014). Modelling the rejection of N-nitrosamines by a spiral-wound reverse osmosis system: Mathematical model development and validation, *Journal of Membrane Science*, Vol. 454, pp. 212–219, doi: <https://doi.org/10.1016/j.memsci.2013.12.008>
19. Zaghbani N., Nakajima M., Nabetani Hiroshi, Hafiane A. (2017). Modeling of reverse osmosis flux of aqueous solution containing glucose, *Korean Journal of Chemical Engineering*, Vol. 34, pp. 407–412, doi: <https://doi.org/10.1007/s11814-016-0298-9>
20. Ruiz-García A., Nuez I. (2016). Long-term performance decline in a brackish water reverse osmosis desalination plant. Predictive model for the water permeability coefficient, *Desalination*, Vol. 397, pp. 101–107, doi: <https://doi.org/10.1016/j.desal.2016.06.027>
21. Al-Obaidi M. A., Kara-Zaitri C., Mujtaba I. M. (2016). Development and Validation of N-nitrosamine Rejection Mathematical Model Using a Spiral-wound Reverse Osmosis Process, *Chemical engineering transactions*, Vol. 52, pp. 1129–1134, doi: <https://doi.org/10.3303/CET1652189>
22. Al-Obaidi M.A., Kara-Zaitri C., Mujtaba I.M. (2017). Removal of phenol from wastewater using spiral-wound reverse osmosis process: Model development based on experiment and simulation, *Journal of Water Process Engineering*, Vol. 18, pp. 20–28, doi: <https://doi.org/10.1016/j.jwpe.2017.05.005>
23. Karabelas A. J., Kostoglou M., Koutsou C. P. (2019). Advanced Dynamic Simulation of Membrane Desalination Modules Accounting for Organic Fouling, *Journal of Membrane Science & Research*, Vol. 5, Is. 2, pp. 178–186, doi: <https://doi.org/10.22079/JMSR.2019.94172.1216>



24. Kezia K., Lee J., Hill A. J., Kentish S. E. (2013). Convective transport of boron through a brackish water reverse osmosis membrane, *Journal of Membrane Science*, Vol. 445, pp. 160-169, doi: <https://doi.org/10.1016/j.memsci.2013.05.041>
25. Nir O., Lahav O. (2014). Modeling weak acids' reactive transport in reverse osmosis processes: A general framework and case studies for SWRO, *Desalination*, Vol. 343, pp. 147-153, doi: <https://doi.org/10.1016/j.desal.2013.11.009>
26. Chen C., Qin H. (2019). A Mathematical Modeling of the Reverse Osmosis Concentration Process of a Glucose Solution, *Processes*, Vol. 7(5), 271, doi: <https://doi.org/10.3390/pr7050271>
27. Al-Obaidi M.A., Kara-Zaïtri C., Mujtaba I.M. (2018). Simulation and optimisation of spiral-wound reverse osmosis process for the removal of N-nitrosamine from wastewater. *Chemical Engineering Research and Design*. Vol. 133, pp. 168-182, <https://doi.org/10.1016/j.cherd.2018.03.012>
28. Patroklou G., Sassi K. M., Mujtaba I. M. (2013). Simulation of Boron Rejection by Seawater Reverse Osmosis Desalination, *Chemical engineering transactions*, Vol. 32, pp. 1873-1878, doi: <https://doi.org/10.3303/CET1332313>
29. Arjmandia M., Chenar M. P., Altaee A., Arjmandi A., Peyravi M., Jahanshahi M., Binaeian E. (2020). Caspian seawater desalination and whey concentration through forward osmosis (FO)-reverse osmosis (RO) and FO-FO-RO hybrid systems: Experimental and theoretical study. *Journal of Water Process Engineering*. Vol. 37, 101492, doi: <https://doi.org/10.1016/j.jwpe.2020.101492>
30. Gaublomme D., Strubbe L., Vanoppen M., Torfs E., Mortier S., Cornelissen E., De Gussem B., Verliefde A. Nopens I. (2020). A generic reverse osmosis model for full-scale operation. *Desalination*. Vol. 490, 114509, doi: <https://doi.org/10.1016/j.desal.2020.114509>
31. Ennasri H., Drighil A., Adhiri R., Fahli A., Moussetad M. (2019). Design and Simulation of a Solar Energy System for Desalination of Brackish Water. *Environmental and Climate Technologies*. Vol. 23, Is. 1, pp. 257–276, doi: <https://doi.org/10.2478/rtuect-2019-0017>
32. Al-Alawy A. F., Salih M. H. (2016). Experimental Study and Mathematical Modelling of Zinc Removal by Reverse Osmosis Membranes. *Iraqi Journal of Chemical and Petroleum Engineering*. Vol.17 No.3, pp. 57- 73.
33. Sachit D. E. (2017). Effect of Several Parameters on Membrane Fouling by Using Mathematical Models of Reverse Osmosis Membrane System. *Al-Nahrain Journal for Engineering Sciences*. Vol.20 No.4, pp.864-870.
34. Al-Obaidi M.A., Mujtaba I.M. (2016). Steady state and dynamic modeling of spiral wound wastewater reverse osmosis process. *Computers & Chemical Engineering*. Vol. 90, pp. 278-299, doi: <https://doi.org/10.1016/j.compchemeng.2016.04.001>
35. Al-Obaidi M.A., Kara-Zaïtri C., Mujtaba I.M. (2017). Optimum design of a multi-stage reverse osmosis process for the production of highly concentrated apple juice. *Journal of Food Engineering*. Vol. 214, pp. 47-59. doi: <https://doi.org/10.1016/j.jfoodeng.2017.06.020>
36. Al-Obaidi M.A., Li J-P., Kara-Zaïtri C., Mujtaba I.M. (2017). Optimisation of reverse osmosis based wastewater treatment system for the removal of chlorophenol using genetic algorithms. *Chemical Engineering Journal*. Vol. 316, pp. 91-100. doi: <https://doi.org/10.1016/j.cej.2016.12.096>
37. Al-Obaidi M.A., Kara-Zaïtri C., Mujtaba I.M. (2017). Development of a mathematical model for apple juice compounds rejection in a spiral-wound reverse osmosis process. *Journal of Food Engineering*. Vol. 192, pp.111-121, doi: <https://doi.org/10.1016/j.jfoodeng.2016.08.005>
38. Al-Obaidi M.A., Li J-P., Alsadaie S., Kara-Zaïtri C., Mujtaba I.M. (2018). Modelling and optimisation of a multistage Reverse Osmosis processes with permeate reprocessing and recycling for the removal of N-nitrosodimethylamine from wastewater using Species Conserving Genetic Algorithms. *Chemical Engineering Journal*. Vol. 350, pp. 824-834, doi: <https://doi.org/10.1016/j.cej.2018.06.022>
39. Altaee A. (2012). Computational model for estimating reverse osmosis system design and performance: Part-one binary feed solution. *Desalination*. Vol. 291, pp. 101-105, doi: <https://doi.org/10.1016/j.desal.2012.01.028>
40. Altaee A., Zaragoza G., van Tonningen H. R. (2014). Comparison between Forward Osmosis-Reverse Osmosis and Reverse Osmosis processes for seawater desalination. *Desalination*. Vol. 336, pp. 50-57, doi: <https://doi.org/10.1016/j.desal.2014.01.002>
41. Altaee A., Sharif A., Zaragoza G., Ismail A. F. (2015). Evaluation of FO-RO and PRO-RO designs for power generation and seawater desalination using impaired water feeds. *Desalination*. Vol. pp. 27-35, doi: <https://doi.org/10.1016/j.desal.2014.06.022>
42. Altaee A., Hilal N. (2015). High recovery rate NF-FO-RO hybrid system for inland brackish water treatment. *Desalination*. Vol. 363, pp. 19-25, doi: <https://doi.org/10.1016/j.desal.2014.12.017>
43. Ameri M., Eshaghi M. S. (2016). A novel configuration of reverse osmosis, humidification–dehumidification and flat plate collector: Modeling and exergy analysis. *Applied Thermal Engineering*. Vol. 103, pp. 855-873, doi: <https://doi.org/10.1016/j.applthermaleng.2016.04.047>
44. Barello M., Manca D., Patel R., Mujtaba I.M. (2015). Operation and modeling of RO desalination process in batch mode. *Computers & Chemical Engineering*. Vol. 83, pp. 139-156. doi: <https://doi.org/10.1016/j.compchemeng.2015.05.022>
45. Choi J.-S., Kim J.-T. (2015). Modeling of full-scale reverse osmosis desalination system: Influence of operational parameters. *Journal of Industrial and Engineering Chemistry*. Vol. 21, pp. 261-268, doi: <https://doi.org/10.1016/j.jiec.2014.02.033>
46. Fujioka T., Oshima N., Suzuki R., Price W. E., Nghiem L. D. (2015). Probing the internal structure of reverse osmosis membranes by positron annihilation spectroscopy: Gaining more insight into the transport of water and small solutes. *Journal of Membrane Science*. Vol. 486, pp. 106-118, doi: <https://doi.org/10.1016/j.memsci.2015.02.007>
47. Hung L.-Y., Lue S. J., You J.-H. (2011). Mass-transfer modeling of reverse-osmosis performance on 0.5–2% salty water. *Desalination*. Vol. 265, pp 67-73, doi: <https://doi.org/10.1016/j.desal.2010.07.033>

48. Jbari Y., Abderaf S. (2020). Parametric study to enhance performance of wastewater treatment process, by reverse osmosis-photovoltaic system. *Applied Water Science*. Vol. 10, 217, doi: <https://doi.org/10.1007/s13201-020-01301-4>
49. Jiang A., Biegler L. T., Wang J., Cheng W., Ding Q., Jiangzhou S. (2015). Optimal operations for large-scale seawater reverse osmosis networks. *Journal of Membrane Science*. Vol. 476, pp. 508-524, doi: <https://doi.org/10.1016/j.memsci.2014.12.005>
50. Kim J., Park M., Shon H. K., Kim J. H. (2016). Performance analysis of reverse osmosis, membrane distillation, and pressure-retarded osmosis hybrid processes. *Desalination*. Vol. 380, pp. 85-92, doi: <https://doi.org/10.1016/j.desal.2015.11.019>
51. Álvarez J. R., Antón F. E., Álvarez-García S., Luque S. (2020). Treatment of Aqueous Effluents from Steel Manufacturing with High Thiocyanate Concentration by Reverse Osmosis. *Membranes*. Vol. 10, Is. 12, 437, doi: <https://doi.org/10.3390/membranes10120437>
52. Nir O., Lahav O. (2013). Coupling mass transport and chemical equilibrium models for improving the prediction of SWRO permeate boron concentrations. *Desalination*. Vol. 310, pp. 87-92, doi: <https://doi.org/10.1016/j.desal.2012.09.001>
53. Sundaramoorthy S., Srinivasan G., Murthy D.V.R. (2011). An analytical model for spiral wound reverse osmosis membrane modules: Part I — Model development and parameter estimation. *Desalination*. Vol. 280, Is. 1–3, pp. 403-411, doi: <https://doi.org/10.1016/j.desal.2011.03.047>
54. Gui S., Mai Z., Fu J., Wei Y., Wan J. (2020). Transport Models of Ammonium Nitrogen in Wastewater from Rare Earth Smelteries by Reverse Osmosis Membranes. *Sustainability*. Vol. 12, Is. 15, 6230, doi: <https://doi.org/10.3390/su12156230>
55. Wu X., Hu Y., Wu L., Li H. (2014). Model and Design of Cogeneration System for Different Demands of Desalination Water, Heat and Power Production. *Chinese Journal of Chemical Engineering*. Vol. 22, Is. 3, pp. 330-338, doi: [https://doi.org/10.1016/S1004-9541\(14\)60036-7](https://doi.org/10.1016/S1004-9541(14)60036-7)
56. Mai Z., Gui S., Fu J., Jiang C., Ortega E., Zhao Y., Tu W., Mickols W., Van der Bruggen B. (2019). Activity-derived model for water and salt transport in reverse osmosis membranes: A combination of film theory and electrolyte theory. *Desalination*, Vol. 469, 114094. doi: <https://doi.org/10.1016/j.desal.2019.114094>
57. Filippini G., Al-Obaidi M.A., Manenti F., Mujtaba I.M. (2018). Performance analysis of hybrid system of multi effect distillation and reverse osmosis for seawater desalination via modelling and simulation. *Desalination*, Vol. 448, pp. 21-35, doi: <https://doi.org/10.1016/j.desal.2018.09.010>
58. Al-Obaidi M.A., Alsarayreh A.A., Al-Hroub A.M., Alsadaie S., Mujtaba I.M. (2018). Performance analysis of a medium-sized industrial reverse osmosis brackish water desalination plant. *Desalination*. Vol. 443, pp. 272-284. doi: <https://doi.org/10.1016/j.desal.2018.06.010>
59. Ruiz-García A., de la Nuez Pestana I. (2019). Feed spacer geometries and permeability coefficients. Effect on the performance in BWRO spirral-wound membrane modules. *Water*. Vol. 11, 152. doi: <https://doi.org/10.3390/w11010152>
60. Ruiz-García A., de la Nuez Pestana I. (2018). A computational tool for designing BWRO systems with spiral wound modules. *Desalination*. Vol. 426, pp. 69-77. doi: <http://dx.doi.org/10.1016/j.desal.2017.10.040>
61. Skiborowski M., Mhamdi A., Kraemer K., Marquardt W. (2012). Model-based structural optimization of seawater desalination plants. *Desalination*. Vol. 292, pp. 30-44. doi: <http://dx.doi.org/10.1016/j.desal.2012.02.007>
62. Gautam D. K., Teklu H., Subbiah S. (2020). Analysis of reverse osmosis process in hollow fiber module with and without secondary permeate outlet. *Journal of Water Process Engineering*. Vol. 36, 101336. doi: <https://doi.org/10.1016/j.jwpe.2020.101336>
63. Al-Obaidi M.A., Kara-Zaitri C., Mujtaba I.M. (2018). Performance evaluation of multi-stage and multi-pass reverse osmosis networks for the removal of N-nitrosodimethylamine -D6 (NDMA) from wastewater using model-based techniques. *Journal of Environmental Chemical Engineering*. Vol. 6, Is. 4, pp. 4797-4808. doi: <https://doi.org/10.1016/j.jece.2018.06.014>
64. Gu B. Xu X. Y., Adjiman C. S. (2017). A predictive model for spiral wound reverse osmosis membrane modules: The effect of winding geometry and accurate geometric details. *Computers & Chemical Engineering*. Vol. 96, pp. 248-265. doi: <https://doi.org/10.1016/j.compchemeng.2016.07.029>
65. Efraty A. (2016). CCD series no-22: Recent advances in RO, FO and PRO and their hybrid applications for high recovery desalination of treated sewage effluents. *Desalination*. Vol. 389, pp. 18-38. doi: <http://dx.doi.org/10.1016/j.desal.2016.01.009>
66. Kim J., Park K., Hong S. (2020). Optimization of two-stage seawater reverse osmosis membrane processes with practical design aspects for improving energy efficiency. *Journal of Membrane Science*. Vol. 601, 117889. doi: <https://doi.org/10.1016/j.memsci.2020.117889>
67. Fraidenraich N., de Castro Vilela O., dos Santos Viana M., Gordon J. M. (2016). Improved analytic modeling and experimental validation for brackish-water reverse-osmosis desalination. *Desalination*. Vol. 380, pp.60-65. doi: <http://dx.doi.org/10.1016/j.desal.2015.11.014>
68. M.A., Kara-Zaitri C., Mujtaba I.M. (2019). Performance evaluation of multi-stage reverse osmosis process with permeate and retentate recycling strategy for the removal of chlorophenol from wastewater. *Computers & Chemical Engineering*. Vol. 121, pp. 12-26. doi: <https://doi.org/10.1016/j.compchemeng.2018.08.035>
69. Wang Q., Zhou Z., Li J., Tang Q., Hu Y. (2019). Investigation of the reduced specific energy consumption of the RO-PRO hybrid system based on temperature-enhanced pressure retarded osmosis. *Journal of Membrane Science*. Vol. 581, pp. 439-452. doi: <https://doi.org/10.1016/j.memsci.2019.03.079>
70. Kim J., Park M., Snyder Sh. A., Kim J. H. (2013). Reverse osmosis (RO) and pressure retarded osmosis (PRO) hybrid processes: Model-based scenario study. *Desalination*. Vol. pp. 121-130. doi: <http://dx.doi.org/10.1016/j.desal.2013.05.010>

71. Niewersch C., Rieth C., Hailamariam L., Oriol G. G., Warczok J. (2020). Reverse osmosis membrane element integrity evaluation using imperfection model. *Desalination*. Vol. 476, 114175. doi: <https://doi.org/10.1016/j.desal.2019.114175>
72. Zaidi S.M. J., Fadhilah F., Khan Z., Ismail A.F. (2015). Salt and water transport in reverse osmosis thin film composite seawater desalination membranes. *Desalination*. Vol. 368, pp. 202-213. doi: <http://dx.doi.org/10.1016/j.desal.2015.02.026>
73. Yao S., Ji M. (2020). A small RO and MCDI coupled seawater desalination plant and its performance simulation analysis and optimization. *Processes*. 2020, Vol. 8(8), 944. doi: <https://doi.org/10.3390/pr8080944>
74. Sassi K., Mujtaba I. (2011). Optimal design of reverse osmosis based desalination process with seasonal variation of feed temperature. *Chemical Engineering Transactions*. Vol. 25, pp. 1055-1060. doi: <https://doi.org/10.3303/CET1125176>
75. Sassi K., Mujtaba I. (2011). Optimal design and operation of reverse osmosis desalination process with membrane fouling. *Chemical Engineering Journal*. Vol. 171, Is. 2, pp. 582-593. doi: <https://doi.org/10.1016/j.cej.2011.04.034>
76. Park K., Heo H., Kim D. Y., Yang D. R. (2018). Feasibility study of a forward osmosis/crystallization/reverse osmosis hybrid process with high-temperature operation: Modeling, experiments, and energy consumption. *Journal of Membrane Science*. Vol. 555, pp. 206-219. doi: <https://doi.org/10.1016/j.memsci.2018.03.031>
77. Venkata Swamy B., Madhumala M., Prakasham R.S., Sridhar S. (2013). Nanofiltration of bulk drug industrial effluent using indigenously developed functionalized polyamide membrane. *Chemical Engineering Journal*. Vol. 233, pp. 193-200. doi: <https://doi.org/10.1016/j.cej.2013.08.045>
78. Golnari A., Moradi A., Soltani A. (2013). Effects of different potential functions on modeling of RO membrane performance by use of an advanced model. *Research on Chemical Intermediates*. Vol. 39, pp. 2603-2619. doi: <https://doi.org/10.1007/s11164-012-0784-6>
79. Moradi A., Mojarradi V., Sarcheshmehpour M. (2013). Prediction of RO membrane performances by use of artificial neural network and using the parameters of a complex mathematical model. *Research on Chemical Intermediates*. Vol. 39, pp. 3235-3249. doi: <https://doi.org/10.1007/s11164-012-0835-z>
80. Madsen H. T., Søgaard E. G. (2014). Applicability and modelling of nanofiltration and reverse osmosis for remediation of groundwater polluted with pesticides and pesticide transformation products. *Separation and Purification Technology*. Vol. 125, pp. 111-119. doi: <http://dx.doi.org/10.1016/j.seppur.2014.01.038>
81. Takeuchi Sh., Tazaki A., Miyauchi S., Kajishim T. (2019). A relation between membrane permeability and flow rate at low Reynolds number in circular pipe. *Journal of Membrane Science*. Vol. 582, pp. 91-102. doi: <https://doi.org/10.1016/j.memsci.2019.03.018>
82. Merdaw A.A., Sharif A.O., Derwish G.A.W. (2011). Mass transfer in pressure-driven membrane separation processes, Part I. *Chemical Engineering Journal*. Vol. 168, pp. 215-228. doi: <https://doi.org/10.1016/j.cej.2010.12.071>
83. Rohlf s W., Thiel G. P., Lienhard V J. H. (2016). Modeling reverse osmosis element design using superposition and an analogy to convective heat transfer. *Journal of Membrane Science*. Vol. 512, pp. 38-49. doi: <http://dx.doi.org/10.1016/j.memsci.2016.03.049>
84. Kaviani pour O., Ingram G. D., Vuthaluru H. B. (2017). Investigation into the effectiveness of feed spacer configurations for reverse osmosis membrane modules using Computational Fluid Dynamics. *Journal of Membrane Science*. Vol. 526, pp. 156-171. doi: <http://dx.doi.org/10.1016/j.memsci.2016.12.034>
85. Anqi A. E., Alkhamis N., Oztekin A. (2015). Numerical simulation of brackish water desalination by a reverse osmosis membrane. *Desalination*. Vol. 369, pp. 156-164. doi: <http://dx.doi.org/10.1016/j.desal.2015.05.007>
86. Anqi A. E., Alrehili M., Usta M., Oztekin A. (2016). Numerical analysis of hollow fiber membranes for desalination. *Desalination*. Vol. 398, pp. 39-51. doi: <http://dx.doi.org/10.1016/j.desal.2016.07.019>
87. Anqi A. E., Alkhamis N., Oztekin A. (2016). Steady three dimensional flow and mass transfer analyses for brackish water desalination by reverse osmosis membranes. *International Journal of Heat and Mass Transfer*. Vol. 101, pp. 399-411. doi: <http://dx.doi.org/10.1016/j.ijheatmasstransfer.2016.05.102>
88. Anqi A. E., Alkhamis N., Oztekin A. (2016). Computational study of desalination by reverse osmosis – Three-dimensional analyses. *Desalination*. Vol. 388, pp. 38-49. doi: <http://dx.doi.org/10.1016/j.desal.2016.03.017>
89. Hamdache A., Belkacem M. (2018). Effects of a zero normal-concentration-gradient outflow boundary condition on concentration polarization in a CFD study of a reverse osmosis process. *Journal of the Brazilian Society of Mechanical Sciences and Engineering*. Vol. 40, 507. doi: <https://doi.org/10.1007/s40430-018-1430-z>
90. Jogdand A., Chaudhuri A. (2015). Modeling of concentration polarization and permeate flux variation in a roto-dynamic reverse osmosis filtration system. *Desalination*. Vol. 375, pp. 54-70. doi: <http://dx.doi.org/10.1016/j.desal.2015.07.011>
91. Min J., Zhang B. (2014). Numerical Studies of Convective Mass Transfer Enhancement in a Membrane Channel by Rectangular Winglets. *Chinese Journal of Chemical Engineering*. Vol. 22, pp. 1061-1071. doi: <http://dx.doi.org/10.1016/j.cjche.2014.09.004>
92. Mojab S. M., Pollard A., Pharoah J. G., Beale S. B., Hanff E. S. (2014). Unsteady Laminar to Turbulent Flow in a Spacer-Filled Channel. *Flow, Turbulence and Combustion*. Vol. 92, pp. 563-577. doi: <http://dx.doi.org/10.1007/s10494-013-9514-4>
93. Ratnayake P., Setiawan R., Bao J., Fimbres-Weihs G., Wiley D. E. (2016). Spatio-temporal frequency response analysis of forced slip velocity effect on solute concentration oscillations in a reverse osmosis membrane channel. *Computers & Chemical Engineering*. Vol. 84, pp. 151-161. doi: <http://dx.doi.org/10.1016/j.compchemeng.2015.08.016>
94. Rohlf s W., Lienhard V J. H. (2016). Entrance length effects on Graetz number scaling in laminar duct flows with periodic obstructions: Transport number correlations for spacer-filled membrane channel flows. *International Journal of Heat and Mass Transfer*. Vol. 97, pp. 842-852. doi: <http://dx.doi.org/10.1016/j.ijheatmasstransfer.2016.02.078>

95. Saeed A., Vuthaluru R., Vuthaluru H. B. (2015). Investigations into the effects of mass transport and flow dynamics of spacer filled membrane modules using CFD. *Chemical Engineering Research and Design*. Vol. 93, pp. 79-99. doi: <http://dx.doi.org/10.1016/j.cherd.2014.07.002>
96. Sousa P., Soares A., Monteiro E., Rouboa A. (2014). A CFD study of the hydrodynamics in a desalination membrane filled with spacers. *Desalination*. Vol. 349, pp. 22-30. doi: <http://dx.doi.org/10.1016/j.desal.2014.06.019>
97. Usta M., Anqi A. E., Oztekin A. (2017). Reverse osmosis desalination modules containing corrugated membranes – Computational study. *Desalination*. Vol. 416, pp. 129-139. doi: <http://dx.doi.org/10.1016/j.desal.2017.05.005>
98. Kaufman Y., Kasher R., Lammertink R. G.H., Freger V. (2012). Microfluidic NF/RO separation: Cell design, performance and application. *Journal of Membrane Science*. Vol. 396, pp. 67-73. doi: <http://doi.org/10.1016/j.memsci.2011.12.052>
99. Abdelbaky M. M. A., El-Refae M. M. (2019). A 3D CFD comparative study between torsioned and non-torsioned net-type feed spacer in reverse osmosis. *SN Applied Sciences*. Vol. 1, 1059. doi: <https://doi.org/10.1007/s42452-019-1098-8>
100. Jeong K., Park M., Ohd S., Kim J. H. (2020). Impacts of flow channel geometry, hydrodynamic and membrane properties on osmotic backwash of RO membranes—CFD modeling and simulation. *Desalination*. Vol. 476, 114229. doi: <https://doi.org/10.1016/j.desal.2019.114229>
101. Luo J., Lie M., Heng Y. (2020). A hybrid modeling approach for optimal design of non-woven membrane channels in brackish water reverse osmosis process with high-throughput computation. *Desalination*. Vol. 489, 114463. doi: <https://doi.org/10.1016/j.desal.2020.114463>
102. Bucs Sz.S., Radu A.I., Lavric V., Vrouwenvelder J.S., Picioreanu C. (2014). Effect of different commercial feed spacers on biofouling of reverse osmosis membrane systems: A numerical study. *Desalination*. Vol. 343, pp. 26-37. doi: <http://dx.doi.org/10.1016/j.desal.2013.11.007>
103. Gu B., Adjiman C. S., Xu X. Y. (2017). The effect of feed spacer geometry on membrane performance and concentration polarisation based on 3D CFD simulations. *Journal of Membrane Science*. Vol. 527, pp. 78-91. doi: <http://dx.doi.org/10.1016/j.memsci.2016.12.058>
104. Haaksman V. A., Siddiqui A., Schellenberg C., Kidwell J., Vrouwenvelder J. S., Picioreanu C. (2017). Characterization of feed channel spacer performance using geometries obtained by X-ray computed tomography. *Journal of Membrane Science*. Vol. 522, pp. 124-139. doi: <http://dx.doi.org/10.1016/j.memsci.2016.09.005>
105. Horstmeyer N., Lippert T., Schön D., Schleder F., Picioreanu C., Achterhold K., Pfeiffer F., Drewes J. E. (2018). CT scanning of membrane feed spacers – Impact of spacer model accuracy on hydrodynamic and solute transport modeling in membrane feed channels. *Journal of Membrane Science*. Vol. 564, pp 133-145. doi: <https://doi.org/10.1016/j.memsci.2018.07.006>
106. Gogar R., Vaseghi G., Lipscomb G. (2019). Comparisons of Experimental and Simulated Velocity Fields in Membrane Module Spacers. *Journal of Membrane Science & Research*. Vol. 5, Is. 4, pp. 283-294. doi: <https://doi.org/10.22079/JMSR.2019.101683.1242>
107. Kerdi S., Qamar A., Alpatova A., Vrouwenvelder J. S., Ghaffour N. (2020). Membrane filtration performance enhancement and biofouling mitigation using symmetric spacers with helical filaments. *Desalination*. Vol. 484, pp. 114454. doi: <https://doi.org/10.1016/j.desal.2020.114454>
108. Kostoglou M., Karabelas A. J. (2013). Comprehensive simulation of flat-sheet membrane element performance in steady state desalination. *Desalination*. Vol. 316, pp. 91-102. doi: <http://dx.doi.org/10.1016/j.desal.2013.01.033>
109. Kostoglou M., Karabelas A.J. (2016). Dynamic operation of flat sheet desalination-membrane elements: A comprehensive model accounting for organic fouling. *Computers & Chemical Engineering*. Vol. 93, pp. 1-12. doi: <http://dx.doi.org/10.1016/j.compchemeng.2016.06.001>
110. Koutsou C. P., Karabelas A. J. (2015). A novel retentate spacer geometry for improved spiral wound membrane (SWM) module performance. *Journal of Membrane Science*. Vol. 488, pp. 129-142. doi: <http://dx.doi.org/10.1016/j.memsci.2015.03.064>
111. Lee Y. K., Won Y.-J., Yoo J. H., Ahn K. H., Lee C.-H. (2013). Flow analysis and fouling on the patterned membrane surface. *Journal of Membrane Science*. Vol. 427, pp. 320-325. doi: <http://dx.doi.org/10.1016/j.memsci.2012.10.010>
112. Li M., Bui T., Chao S. (2016). Three-dimensional CFD analysis of hydrodynamics and concentration polarization in an industrial RO feed channel. *Desalination*. Vol. 397, pp. 194-204. doi: <http://dx.doi.org/10.1016/j.desal.2016.07.005>
113. Mansouri N., Moghimi M., Taherinejad M. (2019). Investigation on hydrodynamics and mass transfer in a feed channel of a spiral-wound membrane element using response surface methodology. *Chemical Engineering Research and Design*. Vol. 149, pp. 147-157. doi: <https://doi.org/10.1016/j.cherd.2019.07.006>
114. Shoukat G., Ellahi F., Sajid M., Uddin E. (2020). Computational Study of Zigzag Spacer Design with Elliptical Cross-Section Filaments. *MATEC Web of Conferences*. Vol. 307, 01047. doi: <https://doi.org/10.1051/mateconf/202030701047>
115. Minelli M., Baschetti M. G., Doghieri F. (2011). A comprehensive model for mass transport properties in nanocomposites. *Journal of Membrane Science*. Vol. 381, Is. 1–2, pp. 10-20. doi: <https://doi.org/doi:10.1016/j.memsci.2011.06.036>
116. Motevalian S. P., Borhan A., Zhou H., Zydny A. (2016). Twisted hollow fiber membranes for enhanced mass transfer. *Journal of Membrane Science*. Vol. 514, pp. 586-594. doi: <http://dx.doi.org/10.1016/j.memsci.2016.05.027>
117. Park J., Lee K. S. (2017). A two-dimensional model for the spiral wound reverse osmosis membrane module. *Desalination*. Vol. 416, pp. 157-165. doi: <http://dx.doi.org/10.1016/j.desal.2017.05.006>
118. Qamar A., Bucs S., Picioreanu C., Vrouwenvelder J., Ghaffour N. (2019). Hydrodynamic flow transition dynamics in a spacer filled filtration channel using direct numerical simulation. *Journal of Membrane Science*. Vol. 590, 117264. doi: <https://doi.org/10.1016/j.memsci.2019.117264>

119. Ronen A., Lerman S., Ramon G. Z., Dosoretz C. G. (2015). Experimental characterization and numerical simulation of the anti-biofouling activity of nanosilver-modified feed spacers in membrane filtration. *Journal of Membrane Science*. Vol. 475, pp. 320-329. doi: <http://dx.doi.org/10.1016/j.memsci.2014.10.042>
120. Toh K.Y., Liang Y.Y., Lau W.J., Fimbres Weihs G.A. (2020). 3D CFD study on hydrodynamics and mass transfer phenomena for SWM feed spacer with different floating characteristics. *Chemical Engineering Research and Design*. Vol. 159, pp. 36-46. doi: <https://doi.org/10.1016/j.cherd.2020.04.010>
121. Usta M., Morabito M., Anqi A., Alrehili M., Hakim A., Oztekin A. (2018). Twisted hollow fiber membrane modules for reverse osmosis-driven desalination. *Desalination*. Vol. 441, pp. 21-34. doi: <https://doi.org/10.1016/j.desal.2018.04.027>
122. Qi J., Lv J., Li Z., Bian W., Li J., Liu S. (2020). A Numerical Simulation of Membrane Distillation Treatment of Mine Drainage by Computational Fluid Dynamics. *Water*. Vol. 12, Is. 12., 3403. doi: <https://doi.org/10.3390/w12123403>
123. Xie P., Murdoch L. C., Ladner D. A. (2014). Hydrodynamics of sinusoidal spacers for improved reverse osmosis performance. *Journal of Membrane Science*. Vol. 453, pp. 92-99. doi: <http://dx.doi.org/10.1016/j.memsci.2013.10.068>
124. Yang Zh., Cheng J., Yang C., Liang B. (2016). CFD-based optimization and design of multi-channel inorganic membrane tubes. *Chinese Journal of Chemical Engineering*. Vol. 24, Is. 10, pp. 1375-1385. doi: <http://dx.doi.org/10.1016/j.cjche.2016.05.044>
125. Zhuang L., Guo H., Wang P., Dai G. (2015). Study on the flux distribution in a dead-end outside-in hollow fiber membrane module. *Journal of Membrane Science*. Vol. 495, pp. 372-383. doi: <http://dx.doi.org/10.1016/j.memsci.2015.07.060>
126. Zhuang L., Guo H., Dai G., Xu Z. (2017). Effect of the inlet manifold on the performance of a hollow fiber membrane module-A CFD study. *Journal of Membrane Science*. Vol. 526, pp. 73-93. doi: <http://dx.doi.org/10.1016/j.memsci.2016.12.018>
127. Uppu A., Chaudhuri A., Das Sh. P., Prakash N. (2020). CFD modeling of gypsum scaling in cross-flow RO filters using moments of particle population balance. *Journal of Environmental Chemical Engineering*. Vol. 8, Is. 5, 104151. doi: <https://doi.org/10.1016/j.jece.2020.104151>
128. Liang Y.Y., Fimbres Weihs G.A., Fletcher D.F. (2018). CFD study of the effect of unsteady slip velocity waveform on shear stress in membrane systems. *Chemical Engineering Science*. Vol. 192, pp. 16-24. doi: <https://doi.org/10.1016/j.ces.2018.07.009>
129. Liang Y.Y., Fimbres Weihs G.A., Wiley D.E. (2020). Comparison of oscillating flow and slip velocity mass transfer enhancement in spacer-filled membrane channels: CFD analysis and validation. *Journal of Membrane Science*. Vol. 593, 117433. doi: <https://doi.org/10.1016/j.memsci.2019.117433>
130. Liang Y.Y., Toh K.Y., Fimbres Weihs G.A. (2019). 3D CFD study of the effect of multi-layer spacers on membrane performance under steady flow. *Journal of Membrane Science*. Vol. 580, pp. 256-267. doi: <https://doi.org/10.1016/j.memsci.2019.02.015>
131. Lim S.Y., Liang Y.Y., Fimbres Weihs G.A., Wiley D.E., Fletcher D.F. (2018). A CFD study on the effect of membrane permeance on permeate flux enhancement generated by unsteady slip velocity. *Journal of Membrane Science*. Vol. 556, pp. 138-145. doi: <https://doi.org/10.1016/j.memsci.2018.03.070>
132. Onorato C., Gaedtker M., Kespe M., Nirschl H., Schäfer A. I. (2019). Renewable energy powered membrane technology: Computational fluid dynamics evaluation of system performance with variable module size and fluctuating energy. *Separation and Purification Technology*. Vol. 220, pp. 206-216. doi: <https://doi.org/10.1016/j.seppur.2019.02.041>
133. Qi B., Wang Y., Wang Z., Zhang Y., Xu Sh., Wang Sh. (2013). Theoretical Investigation on Internal Leakage and Its Effect on the Efficiency of Fluid Switcher-Energy Recovery Device for Reverse Osmosis Desalting Plant. *Chinese Journal of Chemical Engineering*. Vol. 21, Is. 11, pp. 1216-1223. doi: [https://doi.org/10.1016/S1004-9541\(13\)60625-4](https://doi.org/10.1016/S1004-9541(13)60625-4)
134. Foo K., Liang Y.Y., Fimbres Weihs G.A. (2020). CFD study of the effect of SWM feed spacer geometry on mass transfer enhancement driven by forced transient slip velocity. *Journal of Membrane Science*. Vol. 597, 117643. doi: <https://doi.org/10.1016/j.memsci.2019.117643>
135. Gruber M. F., Aslak U., Hélix-Nielsen C. (2016). Open-source CFD model for optimization of forward osmosis and reverse osmosis membrane modules. *Separation and Purification Technology*. Vol. 158, pp. 183-192. doi: <http://dx.doi.org/10.1016/j.seppur.2015.12.017>
136. Ahmed S., Taif Seraji M., Jahedi J., Hashi M.A. (2012). Application of CFD for simulation of a baffled tubular membrane. *Chemical Engineering Research and Design*. Vol. 90, Is. 5, pp. 600-608. doi: <http://dx.doi.org/doi:10.1016/j.cherd.2011.08.024>
137. Haddadi B., Jordan C., Miltner M., Harasek M. (2018). Membrane modeling using CFD: Combined evaluation of mass transfer and geometrical influences in 1D and 3D. *Journal of Membrane Science*. Vol. 563, pp. 199-209. doi: <https://doi.org/10.1016/j.memsci.2018.05.040>
138. Kaya R., Deveci G., Turken T., Sengur R., Guclu S., Koseoglu-Imer D.Y., Koyuncu I. (2014). Analysis of wall shear stress on the outside-in type hollow fiber membrane modules by CFD simulation. *Desalination*. Vol. 351, pp. 109-119. doi: <http://dx.doi.org/10.1016/j.desal.2014.07.033>
139. Wu S.-E., Lin Y.-Ch., Hwang K.-J., Cheng T.-W., Tung K.-L. (2018). High-efficiency hollow fiber arrangement design to enhance filtration performance by CFD simulation. *Chemical Engineering and Processing - Process Intensification*. Vol. 125, pp. 87-96. doi: <https://doi.org/10.1016/j.cep.2018.01.003>
140. Li W., Su X., Palazzolo A., Ahmed Sh., Thomas E. (2017). Reverse osmosis membrane, seawater desalination with vibration assisted reduced inorganic fouling. *Desalination*. Vol. 417, pp. 102-114. doi: <http://dx.doi.org/10.1016/j.desal.2017.05.016>
141. Kaviani-pour O., Ingram G. D., Vuthaluru H. B. (2019). Studies into the mass transfer and energy consumption of commercial feed spacers for RO membrane modules using CFD: Effectiveness of performance measures. *Chemical Engineering Research and Design*. Vol. 141, pp. 328-338. doi: <https://doi.org/10.1016/j.cherd.2018.10.041>

142. Naskar M., Rana K., Chatterjee D., Dhara T., Sultana R., Sarkar D. (2019). Design, performance characterization and hydrodynamic modeling of intermeshed spinning basket membrane (ISBM) module. *Chemical Engineering Science*. Vol. 206, pp. 446-462. doi: <https://doi.org/10.1016/j.ces.2019.05.049>
143. Ahmed I., Hussain A., Hasani S.M.F., Shakaib M., Yunus R. M. (2012). Computational modeling for visualization of flow patterns in a membrane testing device. *Separation and Purification Technology*. Vol. 90, pp. 1-9. doi: <https://doi.org/doi:10.1016/j.seppur.2012.02.004>
144. Chaumeil F., Crapper M. (2013). DEM simulations of initial deposition of colloidal particles around non-woven membrane spacers. *Journal of Membrane Science*. Vol. 442, pp. 254-263. doi: <http://dx.doi.org/10.1016/j.memsci.2013.04.031>
145. Saeed A., Vuthaluru R., Yang Y., Vuthaluru H. B. (2012). Effect of feed spacer arrangement on flow dynamics through spacer filled membranes. *Desalination*. Vol. 285, pp. 163-169. doi: <https://doi.org/10.1016/j.desal.2011.09.050>
146. Fimbres Weihs G.A., Wiley D.E. (2014). CFD analysis of tracer response technique under cake-enhanced osmotic pressure. *Journal of Membrane Science*. Vol. 449, pp. 38-49. doi: <http://dx.doi.org/10.1016/j.memsci.2013.08.015>
147. Srivathsan G., Sparrow E. M., Gorman J. M. (2014). Reverse osmosis issues relating to pressure drop, mass transfer, turbulence, and unsteadiness. *Desalination*. Vol. 341, pp. 83-86. doi: <https://doi.org/10.1016/j.desal.2014.02.021>
148. Wypyssek D., Rall D., Wiese M., Neef T., Koops G.-H., Wessling M. (2019). Shell and lumen side flow and pressure communication during permeation and filtration in a multibore polymer membrane module. *Journal of Membrane Science*. Vol. 584, pp. 254-267. doi: <https://doi.org/10.1016/j.memsci.2019.04.070>
149. Taherinejad M., Moghimi M., Derakhshan Sh. (2019). Hydrodynamic modeling of the spiral-wound membrane module including the membrane curvature: reverse osmosis case study. *Korean Journal of Chemical Engineering*. Vol. 36, pp. 2074-2084. doi: <https://doi.org/10.1007/s11814-019-0372-1>
150. Ligaray M., Kim N.-H., Park S., Park J.-S., Park J. Kim Y., Cho K. H. (2020). Energy projection of the seawater battery desalination system using the reverse osmosis system analysis model. *Chemical Engineering Journal*. Vol. 395, pp. 125082. doi: <https://doi.org/10.1016/j.cej.2020.125082>
151. Taherinejad M., Derakhshan Sh., Yavarinasab A. (2017). Hydrodynamic analysis of spiral wound reverse osmosis membrane recovery fraction and permeate water flow rate. *Desalination*. Vol. 411, pp. 59-68. doi: <http://dx.doi.org/10.1016/j.desal.2017.02.009>
152. Nejati S., Mirbagheri S. A., Warsinger D. M., Fazeli M. (2019). Biofouling in seawater reverse osmosis (SWRO): Impact of module geometry and mitigation with ultrafiltration. *Journal of Water Process Engineering*. Vol. 29, 100782. doi: <https://doi.org/10.1016/j.jwpe.2019.100782>
153. Johannink M., Masilamani K., Mhamdi A., Roller S., Marquardt W. (2015). Predictive pressure drop models for membrane channels with non-woven and woven spacers. *Desalination*. Vol. 376, pp. 41-54. doi: <http://dx.doi.org/10.1016/j.desal.2015.07.024>
154. Palomar P., Lara J.L., Losada I.J., Rodrigo M., Álvarez A. (2012). Near field brine discharge modelling part 1: Analysis of commercial tools. *Desalination*. Vol. 290, pp. 14-27. doi: <https://doi.org/10.1016/j.desal.2011.11.037>
155. Haidaria A.H., Heijman S.G.J., van der Meer W.G.J. (2018). Optimal design of spacers in reverse osmosis. *Separation and Purification Technology*. Vol. 192, pp. 441-456. doi: <https://doi.org/10.1016/j.seppur.2017.10.042>
156. Karabelas A.J., Koutsou C.P., Kostoglou M. (2014). The effect of spiral wound membrane element design characteristics on its performance in steady state desalination — A parametric study. *Desalination*. Vol. 332, Is. 1, 2 pp. 76-90. doi: <http://dx.doi.org/10.1016/j.desal.2013.10.027>
157. Koutsou C.P., Karabelas A.J., Kostoglou M. (2014). Membrane desalination under constant water recovery – The effect of module design parameters on system performance. *Separation and Purification Technology*. Vol. 147, pp. 90-113. doi: <http://dx.doi.org/10.1016/j.seppur.2015.04.012>
158. Barello M., Manca D., Patel R., Mujtaba I.M. (2014). Neural network based correlation for estimating water permeability constant in RO desalination process under fouling. *Desalination*. Vol. 345, pp. 101-111. doi: <http://dx.doi.org/10.1016/j.desal.2014.04.016>
159. Farahbakhsh J., Delnavaz M., Vatanpour V. (2019). Simulation and characterization of novel reverse osmosis membrane prepared by blending polypyrrole coated multiwalled carbon nanotubes for brackish water desalination and antifouling properties using artificial neural networks. *Journal of Membrane Science*. Vol. 581, pp. 123-138. doi: <https://doi.org/10.1016/j.memsci.2019.03.050>
160. Salami E. S., Ehteshami M., Karimi-Jashni A., Salari M., Nikbakht Sheibani S., Ehteshami A. (2016). A mathematical method and artificial neural network modeling to simulate osmosis membrane's performance. *Modeling Earth Systems and Environment*. Vol. 2, pp. 1-11. doi: <https://doi.org/10.1007/s40808-016-0261-0>
161. Mohammad A. Th., Al-Obaidi, M. A., Hameed E. M., Basheer B. N., Mujtab I. M. (2020). Modelling the chlorophenol removal from wastewater via reverse osmosis process using a multilayer artificial neural network with genetic algorithm. *Journal of Water Process Engineering*. Vol. 33, 100993. doi: <https://doi.org/10.1016/j.jwpe.2019.100993>
162. Aish A. M., Zaqoot H. A., Abdeljawad S. M. (2015). Artificial neural network approach for predicting reverse osmosis desalination plants performance in the Gaza Strip. *Desalination*. Vol. 367, pp. 240-247. doi: <http://dx.doi.org/10.1016/j.desal.2015.04.008>
163. Jbari Y., Abderaf S. (2020). Parametric study to enhance performance of wastewater treatment process, by reverse osmosis-photovoltaic system. *Applied Water Science*. Vol. 10, 217. doi: <https://doi.org/10.1007/s13201-020-01301-4>

164. Gu J., Luo J., Lif M., Huang C., Heng Y. (2020). Modeling of pressure drop in reverse osmosis feed channels using multilayer artificial neural networks. *Chemical Engineering Research and Design*. Vol. 159, pp. 146-156. doi: <https://doi.org/10.1016/j.cherd.2020.04.019>
165. Rall D., Schweidtmann A. M., Kruse M., Evdochenko E., Mitsos A., Wessling M. (2020). Multi-scale membrane process optimization with high-fidelity ion transport models through machine learning. *Journal of Membrane Science*. Vol. 608, 118208. doi: <https://doi.org/10.1016/j.memsci.2020.118208>
166. Khayet M., Cojocar C., Essalhi M. (2011). Artificial neural network modeling and response surface methodology of desalination by reverse osmosis. *Journal of Membrane Science*. Vol. 368, Is. 1–2, pp. 202-214. doi: <https://doi.org/10.1016/j.memsci.2010.11.030>
167. Park S., Baek S.-S., Pyo J. C. Pachepsky Y., Park J., Cho K. H. (2019). Deep neural networks for modeling fouling growth and flux decline during NF/RO membrane filtration. *Journal of Membrane Science*. Vol. 587, 117164. doi: <https://doi.org/10.1016/j.memsci.2019.06.004>
168. Roehl E. A., Ladner D. A., Daamen R. C., Cook J. B., Safarik J., Phipps D. W., Xie P. (2018). Modeling fouling in a large RO system with artificial neural networks. *Journal of Membrane Science*. Vol. 552, pp. 95-106. doi: <https://doi.org/10.1016/j.memsci.2018.01.064>
169. Cabrera P., Carta J. A., González J., Melián G. (2018). Wind-driven SWRO desalination prototype with and without batteries: A performance simulation using machine learning models. *Desalination*. Vol. 435, pp. 77-96. doi: <https://doi.org/10.1016/j.desal.2017.11.044>
170. Sargolzaei J., Haghghi Asl M., Hedayati Moghaddam A. (2012). Membrane permeate flux and rejection factor prediction using intelligent systems. *Desalination*. Vol. 284, pp. 92-99. doi: <https://doi.org/10.1016/j.desal.2011.08.041>
171. Azamat, J., Khataee, A. Joo, S.W. (2014) Separation of a heavy metal from water through a membrane containing boron nitride nanotubes: molecular dynamics simulations. *Journal of Molecular Modeling*. Vol. 20, 2468. doi: <https://doi.org/10.1007/s00894-014-2468-1>
172. Talati S., Mohebbi A., Dorrani H. (2019). Investigation of the Capability of Carbon Nanotube Membranes in Separating the Heavy Metal Ions from Aqueous Solutions by Molecular Dynamics Simulation. *Journal of Engineering Thermophysics* Vol. 28, pp. 123–137. doi: <https://doi.org/10.1134/S1810232819010107>
173. Hinkle K. R., Wang X., Gu X., Jameson C. J., Murad S. (2018). Computational Molecular Modeling of Transport Processes in Nanoporous Membranes. *Processes*. Vol. 6. Is. 8. 124. doi: <https://doi.org/10.3390/pr6080124>
174. Boateng L. K., Madarshahian R., Yoon Y. Caicedo J. M., Flora J. R. V. (2016). A probabilistic approach for estimating water permeability in pressure-driven membranes. *Journal of Molecular Modeling*. Vol. 22, 185. doi: <https://doi.org/10.1007/s00894-016-3049-2>
175. Gao W., She F., Zhang J., Dumée L. F., He L., Hodgson P. D., Kong L. (2015). Understanding water and ion transport behaviour and permeability through poly(amide) thin film composite membrane. *Journal of Membrane Science*. Vol. 487, pp. 32-39. doi: <https://doi.org/10.1016/j.memsci.2015.03.052>
176. Li J., Kong X., Lu D., Liu Zh. (2015). Italicized carbon nanotube facilitating water transport: a molecular dynamics simulation. *Science Bulletin*. Vol. 60, Is.18, pp. 1580-1586. doi: <https://doi.org/10.1007/s11434-015-0888-7>
177. Shen J.-W., Li J., Liu F., Zhang L., Liang L., Wang H., Wu J.-Y. (2020). A molecular dynamics study on water desalination using single-layer MoSe<sub>2</sub> nanopore. *Journal of Membrane Science*. Vol. 595, 117611. doi: <https://doi.org/10.1016/j.memsci.2019.117611>
178. Zheng B., Tian Y., Jia Sh., Zhao X., Li H. (2020). Molecular dynamics study on applying layered graphene oxide membranes for separating cadmium ions from water. *Journal of Membrane Science*. Vol. 603, 117996. doi: <https://doi.org/10.1016/j.memsci.2020.117996>
179. Shen M., Keten S., Lueptow R. M. (2016). Rejection mechanisms for contaminants in polyamide reverse osmosis membranes. *Journal of Membrane Science*. Vol. 509, pp. 36-47. doi: <https://doi.org/10.1016/j.memsci.2016.02.043>
180. Shen M., Keten S., Lueptow R. M. (2016). Dynamics of water and solute transport in polymeric reverse osmosis membranes via molecular dynamics simulations. *Journal of Membrane Science*. Vol. 506, pp. 95-108. doi: <https://doi.org/10.1016/j.memsci.2016.01.051>
181. Kiat Ng C., Domilongo Bope C., Nalaparaju A., Cheng Y., Lu L., Wang R., Cao B. (2016). Concentrating synthetic estrogen 17 $\alpha$ -ethinyl estradiol using microporous polyethersulfone hollow fiber membranes: Experimental exploration and molecular simulation. *Chemical Engineering Journal*. Vol. 314, pp. 80-87. doi: <https://doi.org/10.1016/j.cej.2016.12.109>
182. Li T., Tu Q., Li Sh. (2019). Molecular dynamics modeling of nano-porous centrifuge for reverse osmosis desalination. *Desalination*. Vol. 451, pp. 182-191. doi: <https://doi.org/10.1016/j.desal.2017.09.015>
183. Zhao Z., Jiang J. (2020). POC/PIM-1 mixed-matrix membranes for water desalination: A molecular simulation study. *Journal of Membrane Science*. Vol. 608, 118173. doi: <https://doi.org/10.1016/j.memsci.2020.118173>
184. Luo Y., Harder E., Faibish R. S., Roux B. (2011). Computer simulations of water flux and salt permeability of the reverse osmosis FT-30 aromatic polyamide membrane. *Journal of Membrane Science*. Vol. 384, Is. 1–2, pp. 1-9. doi: <https://doi.org/10.1016/j.memsci.2011.08.057>
185. Lyu Q., Kang D.-Y., Hu S., Lin L.-Ch. (2020). Exploiting interior surface functionalization in reverse osmosis desalination membranes to mitigate permeability–selectivity trade-off: Molecular simulations of nanotube-based membranes. *Desalination*. Vol. 491, 114537. doi: <https://doi.org/10.1016/j.desal.2020.114537>

186. Chen Q., Yang X. (2015). Pyridinic nitrogen doped nanoporous graphene as desalination membrane: Molecular simulation study. *Journal of Membrane Science*. Vol. 496, pp. 108-117. doi: <https://doi.org/10.1016/j.memsci.2015.08.052>
187. Surblys D., Yamada T., Thomsen B., Kawakami T., Shigemoto I., Okabe J., Ogawa T., Kimura M., Sugita Y., Yagi K. (2020). Amide A band is a fingerprint for water dynamics in reverse osmosis polyamide membranes. *Journal of Membrane Science*. Vol. 596, 117705. doi: <https://doi.org/10.1016/j.memsci.2019.117705>
188. Ji W.M., Zhang L.W. (2019). Molecular dynamics simulations of water desalination through polymerized fullerite membrane. *Journal of Membrane Science*. Vol. 576, pp. 108-115. doi: <https://doi.org/10.1016/j.memsci.2019.01.028>
189. Yao Y., Li M., Cao X., Zhang P., Zhang W., Zheng J., Zhang X., Wang L. (2018). A novel sulfonated reverse osmosis membrane for seawater desalination: Experimental and molecular dynamics studies. *Journal of Membrane Science*. Vol. 550, pp. 470-479. doi: <https://doi.org/10.1016/j.memsci.2018.01.023>
190. Tomohisa Y., Kotaka K., Nakagawa K., Shintani T., Wu H.-Ch., Matsuyama H., Fujimura Y., Kawakatsu T. (2018). Molecular dynamics simulation study of polyamide membrane structures and RO/FO water permeation properties. *Membranes*. Vol. 8, Is. 4, 127. doi: <https://doi.org/10.3390/membranes8040127>
191. Rizzuto C., Pugliese G., Bahattab M. A., Aljlil S. A., Drioli E., Tocci E. (2018). Multiwalled carbon nanotube membranes for water purification. *Separation and Purification Technology*. Vol. 193, pp. 378-385. doi: <https://doi.org/10.1016/j.seppur.2017.10.025>
192. Ding M., Szymczyk A., Goujon F., Soldera A., Ghof A. (2014). Structure and dynamics of water confined in a polyamide reverse-osmosis membrane: A molecular-simulation study. *Journal of Membrane Science*. Vol. 458, pp. 236-244. doi: <http://dx.doi.org/10.1016/j.memsci.2014.01.054>
193. Ding M., Ghoufi A., Anthony S. (2014). Molecular simulations of polyamide reverse osmosis membranes. *Desalination*. Vol. 343, pp. 48-53. doi: <https://doi.org/10.1016/j.desal.2013.09.024>
194. Ding M., Szymczyk A., Ghof A. (2015). On the structure and rejection of ions by a polyamide membrane in pressure-driven molecular dynamics simulations. *Desalination*. Vol. 368, pp. 76-80. doi: <http://dx.doi.org/10.1016/j.desal.2015.01.003>
195. Ding M., Szymczyk A., Ghof A. (2016). Hydration of a polyamide reverse-osmosis membrane. *Journal of Membrane Science*. Vol. 501, pp. 248-253. doi: <http://dx.doi.org/10.1016/j.memsci.2015.12.036>
196. Azamat J., Baghban N. B., Erfan-Niya H. (2020). Atomistic understanding of functionalized  $\gamma$ -graphyne-1 nanosheet membranes for water desalination. *Journal of Membrane Science*. Vol. 604, 118079. doi: <https://doi.org/10.1016/j.memsci.2020.118079>
197. Yang H., Baek J., Park H. G. (2020). Architecture and mass transport properties of graphene-based membranes. *JMST Advances*. Vol. 2, pp. 77-88. doi: <https://doi.org/10.1007/s42791-020-00032-6>
198. Zhu Y., Zhou J., Lu X., Guo X., Lu L. (2013). Molecular simulations on nanoconfined water molecule behaviors for nanoporous material applications. *Microfluidics and Nanofluidics*. Vol. 15, pp. 191-205. doi: <https://doi.org/10.1007/s10404-013-1143-7>
199. Müller E. A. (2013). Purification of water through nanoporous carbon membranes: a molecular simulation viewpoint. *Current Opinion in Chemical Engineering*. Vol. 2, Is. 2, pp. 223-228. doi: <http://dx.doi.org/10.1016/j.coche.2013.02.004>
200. Nguyen Ch. Th., Beskok A. (2020). Water desalination performance of h-BN and optimized charged graphene membranes. *Microfluidics and Nanofluidics*. Vol. 24, 39. doi: <https://doi.org/10.1007/s10404-020-02340-8>
201. Song Y., Wei M., Xu F., Wang Y. (2020). Molecular simulations of water transport resistance in polyamide RO membranes: interfacial and interior contributions. *Engineering*. Vol. 6, Is. 5, pp. 577-584. doi: <https://doi.org/10.1016/j.eng.2020.03.008>
202. Karavas Ch.-S., Arvanitis K. G., Papadakis G. (2019). Optimal technical and economic configuration of photovoltaic powered reverse osmosis desalination systems operating in autonomous mode. *Desalination*. Vol. 466, pp. 97-106. doi: <https://doi.org/10.1016/j.desal.2019.05.007>
203. Atia A. A., Fthenakis V. (2019). Active-salinity-control reverse osmosis desalination as a flexible load resource. *Desalination*. Vol. 468, 114062. doi: <https://doi.org/10.1016/j.desal.2019.07.002>
204. Al-Obaidi M.A., Kara-Zaitri C., Mujtaba I.M. (2019). Economic removal of chlorophenol from wastewater using multi-stage spiral-wound reverse osmosis process: Simulation and optimisation. *Journal of Water Process Engineering*. Vol. 31, 100829. doi: <https://doi.org/10.1016/j.jwpe.2019.100829>
205. Abejón A., Garea A., Irabien A. (2015). Arsenic removal from drinking water by reverse osmosis: Minimization of costs and energy consumption. *Separation and Purification Technology*. Vol. 144, pp. 46-53. doi: <https://doi.org/10.1016/j.seppur.2015.02.017>
206. Alnouri S., Linke P. (2013). Optimal SWRO network synthesis and design assessment with water quality insights. *Chemical Engineering Transactions*. Vol. 35, pp. 1225-1230. doi: <https://doi.org/10.3303/CET1335204>
207. Alnouri S. Y., Linke P. (2013). Optimal SWRO desalination network synthesis using multiple water quality parameters. *Journal of Membrane Science*. Vol. 444, pp. 493-512. doi: <https://doi.org/10.1016/j.memsci.2013.04.066>
208. Alnouri S. Y., Linke P. (2014). Optimal seawater reverse osmosis network design considering product water boron specifications. *Desalination*. Vol. 345, pp. 112-127. doi: <https://doi.org/10.1016/j.desal.2014.04.030>
209. Jiang A., Wang J., Biegler L. T., Cheng W., Xing Ch., Jiang Zh. (2015). Operational cost optimization of a full-scale SWRO system under multi-parameter variable conditions. *Desalination*. Vol. 355, pp. 124-140. doi: <https://doi.org/10.1016/j.desal.2014.10.016>
210. Xu D., Acker T., Zhang X. (2019). Size optimization of a hybrid PV/wind/diesel/battery power system for reverse osmosis desalination. *Journal of Water Reuse and Desalination*. Vol. 9, Is. 4, pp. 405-422. doi: <https://doi.org/10.2166/wrd.2019.019>



211. Khor Ch. S., Chachuat B., Shah N. (2012). A superstructure optimization approach for water network synthesis with membrane separation-based regenerators. *Computers & Chemical Engineering*. Vol. 42, pp. 48-63. doi: <https://doi.org/10.1016/j.compchemeng.2012.02.020>
212. Maalouf S., Rosso D., Yeh W. W.-G. (2014). Optimal planning and design of seawater RO brine outfalls under environmental uncertainty. *Desalination*. Vol. 333, Is. 1, pp. 134-145. doi: <https://doi.org/10.1016/j.desal.2013.11.015>
213. Maleki A. (2018). Design and optimization of autonomous solar-wind-reverse osmosis desalination systems coupling battery and hydrogen energy storage by an improved bee algorithm. *Desalination*. Vol. 435, pp. 221-234. doi: <https://doi.org/10.1016/j.desal.2017.05.034>
214. Malik S. N., Bahri P. A., Vu L. T.T. (2016). Steady state optimization of design and operation of desalination systems using Aspen Custom Modeler. *Computers & Chemical Engineering*. Vol. 91, pp. 247-256. doi: <https://doi.org/10.1016/j.compchemeng.2016.04.024>
215. Toth A. J. (2020). Modelling and optimisation of multi-stage flash distillation and reverse osmosis for desalination of saline process wastewater sources. *Membranes*. Vol. 10, Is. 10, 265. doi: <https://doi.org/10.3390/membranes10100265>
216. Peng W., Maleki A., Rosend M. A., Azarikhah P. (2018). Optimization of a hybrid system for solar-wind-based water desalination by reverse osmosis: Comparison of approaches. *Desalination*. Vol. 442, pp. 16-31. doi: <https://doi.org/10.1016/j.desal.2018.03.021>
217. Prathapaneni D. R., Detroja K. (2020). Optimal design of energy sources and reverse osmosis desalination plant with demand side management for cost-effective freshwater production. *Desalination*. Vol. 496, 114741. doi: <https://doi.org/10.1016/j.desal.2020.114741>
218. Sassi K. M., Mujtaba I. M. (2013). MINLP based superstructure optimization for boron removal during desalination by reverse osmosis. *Journal of Membrane Science*. Vol. 440, pp. 29-39. doi: <https://doi.org/10.1016/j.memsci.2013.03.012>
219. Senthil S., Senthilmurugan S. (2016). Reverse Osmosis–Pressure Retarded Osmosis hybrid system: Modelling, simulation and optimization. *Desalination*. Vol. 389, pp. 78-97. doi: <https://doi.org/10.1016/j.desal.2016.01.027>
220. Zebbar M., Messlem Y., Gouichiche A., Tadjine M. (2019). Super-twisting sliding mode control and robust loop shaping design of RO desalination process powered by PV generator. *Desalination*. Vol. 458, pp. 122-135. doi: <https://doi.org/10.1016/j.desal.2019.02.011>
221. Ruiz-García A., Nuez I., Carrascosa-Chisvert M.D., Santana J.J. (2020). Simulations of BWRO systems under different feedwater characteristics. Analysis of operation windows and optimal operating points. *Desalination*. Vol. 491, 114582. doi: <https://doi.org/10.1016/j.desal.2020.114582>
222. Jiang A., Wang J., Cheng W., Xing Ch., Jiangzhou Sh. (2014). A Dynamic Optimization Strategy for the Operation of Large Scale Seawater Reverses Osmosis System. *Mathematical Problems in Engineering*. Volume 2014, ID 635434. doi: <https://doi.org/10.1155/2014/635434>
223. Bdour M., Dalala Z., Al-Addous M., Kharabsheh A., Khzouz H. (2020). Mapping RO-Water Desalination System Powered by Standalone PV System for the Optimum Pressure and Energy Saving. *Applied Sciences*. Vol. 10, Is. 6, 2161. doi: <https://doi.org/10.3390/app10062161>
224. Bitaw T. N., Park K., Yang D. R. (2016). Optimization on a new hybrid Forward osmosis-Electrodialysis-Reverse osmosis seawater desalination process. *Desalination*. Vol. 398, pp. 265-281. doi: <https://doi.org/10.1016/j.desal.2016.07.032>
225. Dimitriou E., Boutikos P., Mohamed E. Sh., Koziel S., Papadakis G. (2017). Theoretical performance prediction of a reverse osmosis desalination membrane element under variable operating conditions. *Desalination*. Vol. 419, pp. 70-78. doi: <https://doi.org/10.1016/j.desal.2017.06.001>
226. Kim J., Hong S. (2018). Optimizing seawater reverse osmosis with internally staged design to improve product water quality and energy efficiency. *Journal of Membrane Science*. Vol. 568, pp. 76-86. doi: <https://doi.org/10.1016/j.memsci.2018.09.046>
227. Li M. (2012). Optimal plant operation of brackish water reverse osmosis (BWRO) desalination. *Desalination*. Vol. 293, pp. 61-68. doi: <https://doi.org/10.1016/j.desal.2012.02.024>
228. Weaver N. J., Wilkin G. S., Morison K. R., Watson M. J. (2020). Minimizing the energy requirements for the production of maple syrup. *Journal of Food Engineering*. Vol. 273, 109823. doi: <https://doi.org/10.1016/j.jfoodeng.2019.109823>
229. Almansoori A., Saif Y. (2014). Structural optimization of osmosis processes for water and power production in desalination applications. *Desalination*. Vol. 344, pp. 12-27. doi: <https://doi.org/10.1016/j.desal.2014.03.002>
230. Al-Aboosi F. Y., El-Halwagi M. M. (2019). A Stochastic Optimization Approach to the Design of Shale Gas/Oil Wastewater Treatment Systems with Multiple Energy Sources under Uncertainty. *Sustainability*. Vol. 11, Is. 18, 4865. doi: <https://doi.org/10.3390/su11184865>
231. Blankert B., Kim Y., Vrouwenvelder H., Ghaffour N. (2020). Facultative hybrid RO-PRO concept to improve economic performance of PRO: Feasibility and maximizing efficiency. *Desalination*. Vol. 478, 114268. doi: <https://doi.org/10.1016/j.desal.2019.114268>
232. Nematzadeh, M., Samimi, A., Shokrollahzadeh, S., Mohebbi-Kalhari, D. (2019). Bentazon removal from aqueous solution by reverse osmosis; optimization of effective parameters using response surface methodology. *Advances in Environmental Technology*. Vol. 5, Is. 4, pp. 193-201. doi: <https://doi.org/10.22104/aet.2020.4228.1209>
233. Al-Obaidi M.A., Kara-Zaitri C., Mujtaba I.M. (2018). Simulation and optimisation of a two-stage/two-pass reverse osmosis system for improved removal of chlorophenol from wastewater. *Journal of Water Process Engineering*. Vol. 22, pp. 131-137. doi: <https://doi.org/10.1016/j.jwpe.2018.01.012>

234. Emamjome A., Zahedi M. M., Ziyaadini M. (2019). Economic analysis for process optimization of Chabahar Maritime University reverse osmosis desalination plant: a case study. *Applied Water Science*. Vol. 9, 114. doi: <https://doi.org/10.1007/s13201-019-0995-8>
235. Mirghaderi F., Rahmanian N., Patel R., Manca D., Mujtaba I. M. (2017). Simulation and Optimization of a Continuous Reverse Osmosis Desalination Process for Making Fresh Water. *Chemical Engineering Transactions*. Vol. 61, pp. 1783-1788. doi: <https://doi.org/10.3303/CET1761295>
236. Emad A., Ajbar A., Almutaz I. (2012). Periodic control of a reverse osmosis desalination process. *Journal of Process Control*. Vol. 22, Is. 1, pp. 218-227. doi: <https://doi.org/10.1016/j.jprocont.2011.09.001>
237. Kelley L. C., Dubowsky S. (2013). Thermal control to maximize photovoltaic powered reverse osmosis desalination systems productivity. *Desalination*. Vol. 314, pp. 10-19. doi: <https://doi.org/10.1016/j.desal.2012.11.036>
238. Volpin F., Fons E., Chekli L., Kim J. E., Jang A., Shon H. K. (2018). Hybrid forward osmosis-reverse osmosis for wastewater reuse and seawater desalination: Understanding the optimal feed solution to minimise fouling. *Process Safety and Environmental Protection*. Vol. 117, pp. 523-532. doi: <https://doi.org/10.1016/j.psep.2018.05.006>
239. Peters Ch. D., Hankins N. P. (2019). Osmotically assisted reverse osmosis (OARO): Five approaches to dewatering saline brines using pressure-driven membrane processes. *Desalination*. Vol. 458, pp. 1-13. doi: <https://doi.org/10.1016/j.desal.2019.01.025>
240. Antipova E., Pozo C., Guillén-Gosálbez G., Boer D., Cabeza L.F., Jiménez L. (2015). On the use of filters to facilitate the post-optimal analysis of the Pareto solutions in multi-objective optimization. *Computers & Chemical Engineering*. Vol. 74, pp. 48-58. doi: <https://doi.org/10.1016/j.compchemeng.2014.12.012>
241. Khoshgoftar Manesh M.H., Ghalami H., Amidpour M., Hamed M.H. (2013). Optimal coupling of site utility steam network with MED-RO desalination through total site analysis and exergoeconomic optimization. *Desalination*. Vol. 316, pp. 42-52. doi: <https://doi.org/10.1016/j.desal.2013.01.022>
242. Sadri S., Khoshkhou R.H., Ameri M. (2016). Multi objective optimization of reverse osmosis desalination plant with exergy approach. *Journal of Mechanical Science and Technology*. Vol. 30, pp. 4807-4814. doi: <https://doi.org/10.1007/s12206-016-0953-4>
243. Al-Obaidi M. A., Kara-Zaitri C., Mujtaba I. M. (2018). Statistical-Based Modeling and Optimization of Chlorophenol Removal from Wastewater Using Reverse Osmosis Process. *Chemical Engineering Transactions*. Vol. 70, pp. 2023-2028. doi: <https://doi.org/10.3303/CET1870338>
244. Stillwell A. S., Webber M. E. (2016). Predicting the Specific Energy Consumption of Reverse Osmosis Desalination. *Water*. Vol. 8, Is. 12, 601. doi: <https://doi.org/10.3390/w8120601>
245. Manenti F., Nadezhdin I. S., Goryunov A. G., Kozin K. A., Baydali S. A., Papisidero D., Rossi F., Potemin R. V. (2015). Operational Optimization of Reverse Osmosis Plant Using MPC. *Chemical Engineering Transactions*. Vol. 45, pp. 247-252. doi: <https://doi.org/10.3303/CET1545042>
246. Gong M., Jiang A., Zhang Q., Wang H., Hu J., Lin Y. (2017). An Improved Finite Element Meshing Strategy for Dynamic Optimization Problems. *Mathematical Problems in Engineering*. Vol. 2017, 4829195. doi: <https://doi.org/10.1155/2017/4829195>
247. Patnana N., Pattnaik S., Varshney T., Singh V. P. (2020). Self-Learning Salp Swarm Optimization Based PID Design of Doha RO Plant. *Algorithms*. Vol. 13, Is. 11, 287. doi: <https://doi.org/10.3390/a13110287>
248. Li D., Yang N., Niu R., Qiu H., Xi Y. (2012). FPGA based QDMC control for reverse-osmosis water desalination system. *Desalination*. Vol. 285, pp. 83-90. doi: <https://doi.org/10.1016/j.desal.2011.09.037>
249. Sobana S., Panda R. C. (2014). Modeling and control of reverse osmosis desalination process using centralized and decentralized techniques. *Desalination*. Vol. 344, pp. 243-251. doi: <https://doi.org/10.1016/j.desal.2014.03.014>
250. Ehteram M., Salih S.Q., Yaseen, Z.M. (2020). Efficiency evaluation of reverse osmosis desalination plant using hybridized multilayer perceptron with particle swarm optimization. *Environmental Science and Pollution Research*. Vol. 27, pp. 15278-15291. doi: <https://doi.org/10.1007/s11356-020-08023-9>
251. Jeong K., Park M., Ki S. J., Kim J. H. (2017). A systematic optimization of Internally Staged Design (ISD) for a full-scale reverse osmosis process. *Journal of Membrane Science*. Vol. 540, pp. 285-296. doi: <https://doi.org/10.1016/j.memsci.2017.06.066>
252. Jeong K., Park M., Chong T. H. (2019). Numerical model-based analysis of energy-efficient reverse osmosis (EERO) process: Performance simulation and optimization. *Desalination*. Vol. 453, pp. 10-21. doi: <https://doi.org/10.1016/j.desal.2018.11.021>
253. Fellah B., Benyoucef B., Chermiti A., Belarbi M., Amara S. (2018). Optimal sizing of a hybrid photovoltaic/wind system supplying a desalination unit. *Journal of Engineering Science and Technology*. Vol. 13, No. 6, pp. 1816-1833
254. Ghobeity A., Mitsos A. (2014). Optimal design and operation of desalination systems: new challenges and recent advances. *Current Opinion in Chemical Engineering*. Vol. 6, pp. 61-68. doi: <https://doi.org/10.1016/j.coche.2014.09.008>
255. Sano Y., Mahidul I. (2018) Optimum operating condition of a hollow fiber reverse osmosis desalination system. *Cogent Engineering*. Vol. 5, Is. 1, 1463898. doi: <https://doi.org/10.1080/23311916.2018.1463898>
256. Davies P.A. (2011). A solar-powered reverse osmosis system for high recovery of freshwater from saline groundwater. *Desalination*. Vol. 271, Is. 1-3, pp. 72-79. doi: <https://doi.org/10.1016/j.desal.2010.12.010>
257. Jabari F., Mohammadi-ivatloo B., Mohammadpourfard M. (2019). Robust optimal self-scheduling of potable water and power producers under uncertain electricity prices. *Applied Thermal Engineering*. Vol. 162, 114258. doi: <https://doi.org/10.1016/j.applthermaleng.2019.114258>

258. Sannino D., Sacco O., Chianese A. (2013). Determination of Optimal Operating Condition in Nanofiltration (NF) and Reverse Osmosis (RO) During the Treatment of a Tannery Wastewater Stream. *Chemical Engineering Transactions*. Vol. 32, pp. 1993-1998. doi: <https://doi.org/10.3303/CET1332333>
259. Zhao P., Bai Y., Liu B., Chang H., Cao Y., Fang J. (2019). Process optimization for producing ultrapure water with high resistivity and low total organic carbon. *Process Safety and Environmental Protection*. Vol. 126, pp. 232-241. doi: <https://doi.org/10.1016/j.psep.2019.04.017>
260. Namany S., Al-Ansari T., Govindan R. (2019). Optimisation of the energy, water, and food nexus for food security scenarios. *Computers & Chemical Engineering*. Vol. 129, 106513. doi: <https://doi.org/10.1016/j.compchemeng.2019.106513>
261. Cao Zh., Deng J., Ye F., Garris Ch. A. (2017). Performance Analysis of Thermal Vapor Compression Integrated with Reverse Osmosis Desalination System. *Chemical Engineering Transactions*. Vol. 61, pp. 919-924. doi: <https://doi.org/10.3303/CET1761151>
262. Heidary B., Tavakoli Hashjin T., Ghobadian B., Roshande R. (2019). Performance analysis of hybrid solar-wind RO-MSF desalination system. *Resource-Efficient Technologies*. Vol. 2, pp. 1-16. doi: <https://doi.org/10.18799/24056537/2019/2/184>
263. Heidary B., Tavakoli Hashjin T., Ghobadian B., Roshandel R. (2019). Exergy of a hybrid solar-wind reverse osmosis-MSF desalination system. *Resource-Efficient Technologies*. Vol. 1, pp. 8-19. doi: <https://doi.org/10.18799/24056537/2019/1/227>
264. Lacroix C., Perier-Muzet M., Stitou D. (2019). Dynamic Modeling and Preliminary Performance Analysis of a New Solar Thermal Reverse Osmosis Desalination Process. *Energies*. Vol. 12, Is. 20, 4015. doi: <https://doi.org/10.3390/en12204015>
265. Haryati S., Hamzah A. B., Goh P. S., Abdullah M. S., Ismail A. F., Bustan M. D. (2017). Process intensification of seawater reverse osmosis through enhanced train capacity and module size – Simulation on Lanzarote IV SWRO plant. *Desalination*. Vol. 408, pp. 92-101. doi: <https://doi.org/10.1016/j.desal.2017.01.011>
266. Ling Ch., Wang Y., Min Ch., Zhang Y. (2018). Economic evaluation of reverse osmosis desalination system coupled with tidal energy. *Frontiers in Energy*. Vol. 12, pp. 297–304. doi: <https://doi.org/10.1007/s11708-017-0478-2>
267. García Latorre F. J., Pérez Báez S. O., Gómez Gotor A. (2015). Energy performance of a reverse osmosis desalination plant operating with variable pressure and flow. *Desalination*. Vol. 366, pp. 146-153. doi: <https://doi.org/10.1016/j.desal.2015.02.039>
268. Nayar K. G., Fernandes J., McGovern R. K., Dominguez K. P., McCance A., Al-Anzi B. S., Lienhard V J. H. (2019). Cost and energy requirements of hybrid RO and ED brine concentration systems for salt production. *Desalination*. Vol. 456, pp. 97-120. doi: <https://doi.org/10.1016/j.desal.2018.11.018>
269. Qin M., Deshmukh A., Epszstein R., Patel S. K., Owoseni O. M., Walker W. Sh., Elimelech M. (2019). Comparison of energy consumption in desalination by capacitive deionization and reverse osmosis. *Desalination*. Vol. 455, pp. 100-114. doi: <https://doi.org/10.1016/j.desal.2019.01.003>
270. Nayar K. G., Fernandes J., McGovern R. K., Al-Anzi B. S., Lienhard V J. H. (2019). Cost and energy needs of RO-ED-crystallizer systems for zero brine discharge seawater desalination. *Desalination*. Vol. 457, pp. 115-132. doi: <https://doi.org/10.1016/j.desal.2019.01.015>
271. Koutsou C.P., Kritikos E., Karabelas A.J., Kostoglou M. (2020). Analysis of temperature effects on the specific energy consumption in reverse osmosis desalination processes. *Desalination*. Vol. 476, 114213. doi: <https://doi.org/10.1016/j.desal.2019.114213>
272. Delgado-Torres A. M., García-Rodríguez L., del Moral M. J. (2020). Preliminary assessment of innovative seawater reverse osmosis (SWRO) desalination powered by a hybrid solar photovoltaic (PV) - Tidal range energy system. *Desalination*. Vol. 477, 114247. doi: <https://doi.org/10.1016/j.desal.2019.114247>
273. Arsović M. R., Topić R. M., Komatina M. S., Gojak M. (2015). Thermodynamical research of using solar energy for desalination of seawater. *Thermal Science*. Vol. 19, No. 5, pp. 1709-1721. doi: <https://doi.org/10.2298/TSC1141220074A>
274. Reimers A. S., Webber M. E. (2018). Systems-level thermodynamic and economic analysis of a seawater reverse osmosis desalination plant integrated with a combined cycle power plant. *Texas Water Journal*. Vol. 9, No 1, pp. 82-95. doi: <https://doi.org/10.21423/twj.v9i1.7065>
275. Akhatov J. S. (2016). Energy and Exergy Analysis of Solar PV Powered Reverse Osmosis Desalination. *Applied Solar Energy*. Vol. 52, pp. 265–270. doi: <https://doi.org/10.3103/S0003701X16040034>
276. Alanezi A. A., Altaee A., Sharif A. O. (2020). The effect of energy recovery device and feed flow rate on the energy efficiency of reverse osmosis process. *Chemical Engineering Research and Design*. Vol. 158, pp. 12-23. doi: <https://doi.org/10.1016/j.cherd.2020.03.018>
277. Bartholomew T. V., Mey L., Arena J. T., Siefert N. S., Mauter M. S. (2017). Osmotically assisted reverse osmosis for high salinity brine treatment. *Desalination*. Vol. 421, pp. 3-11. doi: <https://doi.org/10.1016/j.desal.2017.04.012>
278. Chae S. H., Seo J., Kim J., Kim Y. M., Kim J. H. (2018). A simulation study with a new performance index for pressure-retarded osmosis processes hybridized with seawater reverse osmosis and membrane distillation. *Desalination*. Vol. 444, pp. 118-128. doi: <https://doi.org/10.1016/j.desal.2018.07.019>
279. El-Sayed T. A., Abdel Fatah A. A. (2016). Performance of hydraulic turbocharger integrated with hydraulic energy management in SWRO desalination plants. *Desalination*. Vol. 379, pp. 85-92. doi: <https://doi.org/10.1016/j.desal.2015.10.013>
280. Jia X., Klemeš J. J., Varbanov P. S., Alwi Sh. R. W. (2019). Analyzing the Energy Consumption, GHG Emission, and Cost of Seawater Desalination in China. *Energies*. Vol. 12, Is. 3, 463. doi: <https://doi.org/10.3390/en12030463>
281. Castro M., Alcanzare M., Esparcia Jr. E., Oco J. (2020). A Comparative Techno-Economic Analysis of Different Desalination Technologies in Off-Grid Islands. *Energies*. Vol. 13, Is. 9., 2261. doi: <https://doi.org/10.3390/en13092261>

282. Karabelas A.J., Koutsou C.P., Kostoglou M., Sioutopoulos D.C. (2018). Analysis of specific energy consumption in reverse osmosis desalination processes. *Desalination*. Vol. 431, pp. 15-21. doi: <https://doi.org/10.1016/j.desal.2017.04.006>
283. Mazlan N. M., Peshev D., Livingston A. G. (2016). Energy consumption for desalination — A comparison of forward osmosis with reverse osmosis, and the potential for perfect membranes. *Desalination*. Vol. 377, pp. 138-151. doi: <https://doi.org/10.1016/j.desal.2015.08.011>
284. Minhas M.B., Jande Y.A.C., Kim W.S. (2014). Combined reverse osmosis and constant-current operated capacitive deionization system for seawater desalination. *Desalination*. Vol. 344, pp. 299-305. doi: <https://doi.org/10.1016/j.desal.2014.03.043>
285. Segal H., Birnhack L., Nir O., Lahav O. (2018). Intensification and energy minimization of seawater reverse osmosis desalination through high-pH operation: Temperature dependency and second pass implications. *Chemical Engineering and Processing - Process Intensification*. Vol. 131, pp. 84-91. doi: <https://doi.org/10.1016/j.cep.2018.07.009>
286. Lourenço A. B., Carvalho M. (2020). Exergoeconomic and exergoenvironmental analyses of an off-grid reverse osmosis system with internal combustion engine and waste heat recovery. *Chemical Engineering Journal Advances*. Vol. 4, 100056. doi: <https://doi.org/10.1016/j.cej.2020.100056>
287. Muhammad A. J., Qureshi B. A., Zubair S. M. (2017). Exergo-economic analysis of a seawater reverse osmosis desalination plant with various retrofit options. *Desalination*. Vol. 401, pp. 88-98. doi: <https://doi.org/10.1016/j.desal.2016.09.032>
288. Eshoul N. M., Agnew B., Al-Weshahi M. A., Atab M. S. (2015). Exergy Analysis of a Two-Pass Reverse Osmosis (RO) Desalination Unit with and without an Energy Recovery Turbine (ERT) and Pressure Exchanger (PX). *Energies*. Vol. 8, Is. 7, pp. 6910-6925. doi: <https://doi.org/10.3390/en8076910>
289. Islam Sh., Dincer I., Yilbas B. S. (2018). Development of a novel solar-based integrated system for desalination with heat recovery. *Applied Thermal Engineering*. Vol. 129, pp. 1618-1633. doi: <https://doi.org/10.1016/j.applthermaleng.2017.09.028>
290. Mokhtari H., Sepahvand M., Fasihfar A. (2016). Thermoeconomic and exergy analysis in using hybrid systems (GT + MED + RO) for desalination of brackish water in Persian Gulf. *Desalination*. Vol. 399, pp. 1-15. doi: <https://doi.org/10.1016/j.desal.2016.07.044>
291. Sadri S., Ameri M., Khoshkhoo R. H. (2017). Multi-objective optimization of MED-TVC-RO hybrid desalination system based on the irreversibility concept. *Desalination*. Vol. 402, pp. 97-108. doi: <https://doi.org/10.1016/j.desal.2016.09.029>
292. Li Q., Moya W., Esfahani I. J., Rashidi J., Yoo Ch. K. (2017). Integration of reverse osmosis desalination with hybrid renewable energy sources and battery storage using electricity supply and demand-driven power pinch analysis. *Process Safety and Environmental Protection*. Vol. 111, pp. 795-809. doi: <https://doi.org/10.1016/j.psep.2017.09.009>
293. Palenzuela P., Zaragoza G., Alarcón D., Blanco J. (2011). Simulation and evaluation of the coupling of desalination units to parabolic-trough solar power plants in the Mediterranean region. *Desalination*. Vol. 281, pp. 379-387. doi: <https://doi.org/10.1016/j.desal.2011.08.014>
294. Shrivastava A., Rosenberg S., Peery M. (2015). Energy efficiency breakdown of reverse osmosis and its implications on future innovation roadmap for desalination. *Desalination*. Vol. 368, pp. 181-192. doi: <https://doi.org/10.1016/j.desal.2015.01.005>
295. Mansour T. M., Ismail T. M., Ramzy Kh., El-Salam M. A. (2020). Energy recovery system in small reverse osmosis desalination plant: Experimental and theoretical investigations. *Alexandria Engineering Journal*. Vol. 59, Is. 5, pp. 3741-3753. doi: <https://doi.org/10.1016/j.aej.2020.06.030>
296. Mansouri M. T., Amidpour M., Ponce-Ortega J. M. (2019). Optimal integration of organic Rankine cycle and desalination systems with industrial processes: Energy-water-environment nexus. *Applied Thermal Engineering*. Vol. 158, 113740. doi: <https://doi.org/10.1016/j.applthermaleng.2019.113740>
297. Kaya A., Evren Tok M., Koc M. (2019). A Levelized Cost Analysis for Solar-Energy-Powered Sea Water Desalination in The Emirate of Abu Dhabi. *Sustainability*. Vol. 11, Is 6, 1691. doi: <https://doi.org/10.3390/su11061691>
298. Aydiner C., Sen U., Topcu S., Ekinci D., Altinay A. D., Koseoglu-Imer D. Y., Keskinler B. (2014). Techno-economic viability of innovative membrane systems in water and mass recovery from dairy wastewater. *Journal of Membrane Science*. Vol. 458, pp. 66-75. doi: <https://doi.org/10.1016/j.memsci.2014.01.058>
299. He W., Wang Y., Sharif A., Shaheed M. H. (2014). Thermodynamic analysis of a stand-alone reverse osmosis desalination system powered by pressure retarded osmosis. *Desalination*. Vol. 352, pp. 27-37. doi: <https://doi.org/10.1016/j.desal.2014.08.006>
300. Kim J. E., Phuntsho Sh., Chekli L., Choi J. Y., Shon H. K. (2018). Environmental and economic assessment of hybrid FO-RO/NF system with selected inorganic draw solutes for the treatment of mine impaired water. *Desalination*. Vol. 429, pp. 96-104. doi: <https://doi.org/10.1016/j.desal.2017.12.016>
301. Gökçek M. (2018). Integration of hybrid power (wind-photovoltaic-diesel-battery) and seawater reverse osmosis systems for small-scale desalination applications. *Desalination*. Vol. 435, pp. 210-220. doi: <https://doi.org/10.1016/j.desal.2017.07.006>
302. Caldera U., Bogdanov D., Breyer Ch. (2016). Local cost of seawater RO desalination based on solar PV and wind energy: A global estimate. *Desalination*. Vol. 385, pp. 207-216. doi: <https://doi.org/10.1016/j.desal.2016.02.004>
303. Clarke D. P., Al-Abdeli Y. M., Kothapalli G. (2013). The effects of including intricacies in the modelling of a small-scale solar-PV reverse osmosis desalination system. *Desalination*. Vol. 311, pp.127-136. doi: <https://doi.org/10.1016/j.desal.2012.11.006>
304. Ma Q., Lu H. (2011). Wind energy technologies integrated with desalination systems: Review and state-of-the-art. *Desalination*. Vol. 277, Is. 1-3, pp. 274-280. doi: <https://doi.org/10.1016/j.desal.2011.04.041>
305. Hirsimaki C., Outram J. G., Millar G. J., Altaee A. (2020). Process simulation of high pH reverse osmosis systems to facilitate reuse of coal seam gas associated water. *Journal of Environmental Chemical Engineering*. Vol. 8, Is. 5, 104122. doi: <https://doi.org/10.1016/j.jece.2020.104122>

306. Gökçek M., Gökçek Ö. B. (2016). Technical and economic evaluation of freshwater production from a wind-powered small-scale seawater reverse osmosis system (WP-SWRO). *Desalination*. Vol. 381, pp. 47-57. doi: <https://doi.org/10.1016/j.desal.2015.12.004>
307. Al-Obaidi M.A., Filippini G., Manenti F., Mujtaba I.M. (2019). Cost evaluation and optimisation of hybrid multi effect distillation and reverse osmosis system for seawater desalination. *Desalination*. Vol. 456, pp. 136-149. doi: <https://doi.org/10.1016/j.desal.2019.01.019>
308. Filippini G., Al-Obaidi M.A., Manenti F., Mujtaba I.M. (2019). Design and economic evaluation of solar-powered hybrid multi effect and reverse osmosis system for seawater desalination. *Desalination*. Vol. 465, pp.114-125. doi: <https://doi.org/10.1016/j.desal.2019.04.016>
309. Im S. J., Jeong S., Jeong S., Jang A. (2020). Techno-economic evaluation of an element-scale forward osmosis-reverse osmosis hybrid process for seawater desalination. *Desalination*. Vol. 476, 114240. doi: <https://doi.org/10.1016/j.desal.2019.114240>
310. Tobin T., Gustafson R., Bura R., Gough H. L. (2020). Integration of wastewater treatment into process design of lignocellulosic biorefineries for improved economic viability. *Biotechnology for Biofuels*. Vol. 13, 24. doi: <https://doi.org/10.1186/s13068-020-1657-7>
311. Blandin G., Verliefe A. R.D., Tang Ch. Y., Le-Clech P. (2015). Opportunities to reach economic sustainability in forward osmosis–reverse osmosis hybrids for seawater desalination. *Desalination*. Vol. 363, pp. 26-36. doi: <https://doi.org/10.1016/j.desal.2014.12.011>
312. Castel Ch., Favre E. (2018). Membrane separations and energy efficiency. *Journal of Membrane Science*. Vol. 548, pp. 345-357. doi: <https://doi.org/10.1016/j.memsci.2017.11.035>
313. Kook S., Lee Ch., Nguyen Th. T., Lee J., Shon H. K., Kim I. S. (2018). Serially connected forward osmosis membrane elements of pressure-assisted forward osmosis–reverse osmosis hybrid system: Process performance and economic analysis. *Desalination*. Vol. 448, pp. 1-12. doi: <https://doi.org/10.1016/j.desal.2018.09.019>
314. Loutatidou S., Arafat H. A. (2015). Techno-economic analysis of MED and RO desalination powered by low-enthalpy geothermal energy. *Desalination*. Vol. 365, pp. 277-292. doi: <https://doi.org/10.1016/j.desal.2015.03.010>
315. Valizadeh B., Ashtiani F. Z., Fouladitajar A., Dabir B., Baraghani S. S. M.6 Armand S. B., Salari B., Kouchakiniya N. (2015). Scale-up economic assessment and experimental analysis of MF–RO integrated membrane systems in oily wastewater treatment plants for reuse application. *Desalination*. Vol. 374, pp. 31-37. doi: <https://doi.org/10.1016/j.desal.2015.07.017>
316. Bick A., Gillerman L., Manor Y., Oron G. (2012). Economic Assessment of an Integrated Membrane System for Secondary Effluent Polishing for Unrestricted Reuse. *Water*. Vol. 4, Is. 1, pp. 219-236. doi: <https://doi.org/10.3390/w4010219>
317. Edalat A., Hoek E. M. V. (2020). Techno-Economic Analysis of RO Desalination of Produced Water for Beneficial Reuse in California. *Water*. Vol. 12, Is. 7, 1850. doi: <https://doi.org/10.3390/w12071850>
318. Toh K.Y., Liang Y.Y., Lau W.J., Fimbres Weihs G.A. (2020). The techno-economic case for coupling advanced spacers to high-permeance RO membranes for desalination. *Desalination*. Vol. 491, 114534. doi: <https://doi.org/10.1016/j.desal.2020.114534>
319. La Cerva M., Gurreri L., Cipollina A., Tamburini A., Ciofalo M., Micale G. (2019). Modelling and cost analysis of hybrid systems for seawater desalination: Electromembrane pre-treatments for Reverse Osmosis. *Desalination*. Vol. 467, pp. 175-195. doi: <https://doi.org/10.1016/j.desal.2019.06.010>
320. Ghafoor A., Ahmed T., Munir A., Arslan Ch., Ahmad S.A. (2020). Techno-economic feasibility of solar based desalination through reverse osmosis. *Desalination*. Vol. 485, 114464. doi: <https://doi.org/10.1016/j.desal.2020.114464>
321. Castro M. T., Esparcia Jr. E. A., Odulio C. M. F., Ocon J. D. (2019). Technoeconomics of Reverse Osmosis as Demand-Side Management for Philippine Off-Grid Islands. *Chemical Engineering Transactions*. Vol. 76, pp. 1129-1134. doi: <https://doi.org/10.3303/CET1976189>
322. Widiasa I.N., Yoshi L.A. (2016). Techno-Economy Analysis A Small Scale Reverse Osmosis System for Brackish Water Desalination. *International Journal of Science and Engineering*. Vol. 10, Is. 2, pp. 51-57. doi: <https://doi.org/10.12777/ijse.10.2.51-57>
323. Hoveidi H., Vahidi H., CheraghAli S. M. T., Aslemanda A. (2017). Economic Evaluation of RO and MEH *Desalination Units in Iranian South-Eastern Villages*. Vol. 1, Is. 1., pp. 99-112. doi: <https://doi.org/10.22097/EEER.2017.46460>
324. Laissaoui M., Palenzuela P., Sharaf Eldean M. A., Nehari D., Alarcón-Padilla D.-C. (2018). Techno-economic analysis of a stand-alone solar desalination plant at variable load conditions. *Applied Thermal Engineering*. Vol. 133, pp. 659-670. doi: <https://doi.org/10.1016/j.applthermaleng.2018.01.074>
325. Abejon R., Abejon A., Puthai W., Ibrahim S.B., Nagasawa H., Tsuru T., Garea A. (2017). Preliminary techno-economic analysis of non-commercial ceramic and organosilica membranes for hydrogen peroxide ultrapurification. *Chemical Engineering Research and Design*. Vol. 125, pp. 385-397. doi: <https://doi.org/10.1016/j.cherd.2017.07.018>
326. Kumar Sh., Groth A., Vlacic L. (2014). An analytical index for evaluating manufacturing cost and performance of low-pressure hollow fibre membrane systems. *Desalination*. Vol. 332, Is. 1, pp. 44-51. doi: <https://doi.org/10.1016/j.desal.2013.10.013>
327. Ochando-Pulido J. M., Hodaifa G., Victor-Ortega M. D., Martinez-Ferez A. (2013). Performance Modeling and Cost Analysis of a Pilot-Scale Reverse Osmosis Process for the Final Purification of Olive Mill Wastewater. *Membranes*. Vol. 3, Is. 4, pp. 285-297. doi: <https://doi.org/10.3390/membranes3040285>
328. Abraham T., Luthra A. (2011). Socio-economic & technical assessment of photovoltaic powered membrane desalination processes for India. *Desalination*. Vol. 268, Is. 1–3, pp. 238-248. doi: <https://doi.org/10.1016/j.desal.2010.10.035>

329. Idrees M. F. (2020). Performance Analysis and Treatment Technologies of Reverse Osmosis Plant – A case study. *Case Studies in Chemical and Environmental Engineering*. Vol. 2, 100007. doi: <https://doi.org/10.1016/j.cscee.2020.100007>
330. Al-Obaidi M.A., Jarullah A.T., Kara-Zaitri C., Mujtaba I.M. (2018). Simulation of hybrid trickle bed reactor–reverse osmosis process for the removal of phenol from wastewater. *Computers & Chemical Engineering*. Vol. 113, pp. 264-273. doi: <https://doi.org/10.1016/j.compchemeng.2018.03.016>
331. Al-Obaidi M.A., Kara-Zaitri C., Mujtaba I.M. (2019). Evaluation of chlorophenol removal from wastewater using multi-stage spiral-wound reverse osmosis process via simulation. *Computers & Chemical Engineering*. Vol. 130, 106522. doi: <https://doi.org/10.1016/j.compchemeng.2019.106522>
332. Alsarayreh A. A., Al-Obaidi M.A., Al-Hroub A.M., Patel R., Mujtaba I.M. (2020). Performance evaluation of reverse osmosis brackish water desalination plant with different recycled ratios of retentate. *Computers & Chemical Engineering*. Vol. 135, 106729. doi: <https://doi.org/10.1016/j.compchemeng.2020.106729>
333. Riverol C., Pilipovik M.V. (2011). Prediction of the behaviour of the Silt Density Index (SDI) in the Caribbean Seawater and its impact on RO desalination plants. *Desalination*. Vol. 268, Is. 1–3, pp. 262-265. doi: <https://doi.org/10.1016/j.desal.2010.09.049>
334. Venkatesan A. K., Ahmad S., Johnson W., Batista J. R. (2011). Salinity reduction and energy conservation in direct and indirect potable water reuse. *Desalination*. Vol. 272, Is. 1–3, pp. 120-127. doi: <https://doi.org/10.1016/j.desal.2011.01.007>
335. Zhou J., Chang V. W.-C., Fane A. G. (2011). Environmental life cycle assessment of reverse osmosis desalination: The influence of different life cycle impact assessment methods on the characterization results. *Desalination*. Vol. 283, pp. 227-236. doi: <https://doi.org/10.1016/j.desal.2011.04.066>
336. Pascual X., Gu H., Bartman A. R., Zhu A., Rahardianto A., Giralt J., Rallo R., Christofides P. D., Cohen Y. (2013). Data-driven models of steady state and transient operations of spiral-wound RO plant. *Desalination*. Vol. 316, pp. 154-161. doi: <https://doi.org/10.1016/j.desal.2013.02.006>
337. Qian Z., Miedema H., de Smet L.C.P.M., Sudholter E.J.R. (2018). Modelling the selective removal of sodium ions from greenhouse irrigation water using membrane technology. *Chemical Engineering Research and Design*. Vol. 134, pp. 154-161, doi: <https://doi.org/10.1016/j.cherd.2018.03.040>
338. Phuc B. D. H., You S.-S., Lim T.-W., Kim H.-S. (2017). Dynamical analysis and control synthesis of RO desalination process against water hammering. *Desalination*. Vol. 402, pp. 133-142. doi: <https://doi.org/10.1016/j.desal.2016.09.023>
339. Cao Zh., Deng J., Ye F., Garris Jr. Ch. A. (2018). Analysis of a hybrid Thermal Vapor Compression and Reverse Osmosis desalination system at variable design conditions. *Desalination*. Vol. 438, pp. 54-62, doi: <https://doi.org/10.1016/j.desal.2018.03.019>
340. Lu Y., Liao A., Hu Y. (2013) Design of reverse osmosis networks for multiple freshwater production. *Korean Journal of Chemical Engineering*. Vol. 30, pp. 988–996. doi: <https://doi.org/10.1007/s11814-013-0009-8>
341. Qian Zh, Liu X., Yu Zh., Zhang H., Jü Y. (2012). A Pilot-scale Demonstration of Reverse Osmosis Unit for Treatment of Coal-bed Methane Co-produced Water and Its Modeling. *Chinese Journal of Chemical Engineering*. Vol. 20, Is. 2, pp. 302-311. doi: [https://doi.org/10.1016/S1004-9541\(12\)60392-9](https://doi.org/10.1016/S1004-9541(12)60392-9)
342. Salo, A. (2017). Simulation of water purification machine for vending cyber physical systems. *Technology Audit and Production Reserves*, Vol. 2, No. (2)(40), pp. 16–21. doi: <https://doi.org/10.15587/2312-8372.2018.128543>
343. Lucay F., Cisternas L.A., Gálvez E.D. (2015). Global sensitivity analysis for identifying critical process design decisions. *Chemical Engineering Research and Design*. Vol. 103, pp. 74-83. doi: <https://doi.org/10.1016/j.cherd.2015.06.015>
344. Singh S., Henderson R. K., Baker A., Stuetz R. M., Khan S. J. (2012). Characterisation of reverse osmosis permeates from municipal recycled water systems using fluorescence spectroscopy: Implications for integrity monitoring. *Journal of Membrane Science*. Vol. 421–422, pp. 180-189. doi: <https://doi.org/10.1016/j.memsci.2012.07.008>
345. Kim Y. Ch., Min T. (2020). Influence of osmotic mediation on permeation of water in reverse osmosis: Experimental and numerical analysis. *Journal of Membrane Science*. Vol. 595, 117574. doi: <https://doi.org/10.1016/j.memsci.2019.117574>
346. Huang Q., Ma W. (2012). A model of estimating scaling potential in reverse osmosis and nanofiltration systems. *Desalination*. Vol. 288, pp. 40-46. doi: <https://doi.org/10.1016/j.desal.2011.12.007>
347. Kim D.Y., Gu B., Yang D.R. (2013). An explicit solution of the mathematical model for osmotic desalination process. *Korean Journal of Chemical Engineering*. Vol. 30, pp. 1691–1699. doi: <https://doi.org/10.1007/s11814-013-0123-7>
348. Raim V., Srebnik S. (2018). Simulation of osmotic pressure across an amorphous semipermeable membrane. *Journal of Membrane Science*. Vol. 563, pp. 183-190. doi: <https://doi.org/10.1016/j.memsci.2018.05.058>
349. Ochando-Pulido J. M., Martínez-Férez A., Stoller M. (2019). Analysis of the Flux Performance of Different RO/NF Membranes in the Treatment of Agroindustrial Wastewater by Means of the Boundary Flux Theory. *Membranes*. Vol. 9, Is. 1, 2. doi: <https://doi.org/10.3390/membranes9010002>
350. Rivas-Perez R., Sotomayor-Moriano J., Pérez-Zuñiga G., Soto-Angles M. E. (2019). Real-Time Implementation of an Expert Model Predictive Controller in a Pilot-Scale Reverse Osmosis Plant for Brackish and Seawater Desalination. *Applied Sciences*. Vol. 9, Is. 14, 2932. doi: <https://doi.org/10.3390/app9142932>
351. Manheim D. C., Jiang S. C. (2017). Investigation of Algal Biotoxin Removal during SWRO Desalination through a Materials Flow Analysis. *Water*. Vol. 9, Is. 10, 730. doi: <https://doi.org/10.3390/w9100730>
352. Zafra-Cabeza A., Ridao M. A., Camacho E. F. (2011). A mixed integer quadratic programming formulation of risk management for reverse osmosis plants. *Desalination*. Vol. 268, Is. 1–3, pp. 46-54. doi: <https://doi.org/10.1016/j.desal.2010.09.048>

353. Bourouni K. (2013). Availability assessment of a reverse osmosis plant: Comparison between Reliability Block Diagram and Fault Tree Analysis Methods. *Desalination*. Vol. 313, pp. 66-76. doi: <https://doi.org/10.1016/j.desal.2012.11.025>
354. Ramon G. Z., Hoek E. M.V. (2013). Transport through composite membranes, part 2: Impacts of roughness on permeability and fouling. *Journal of Membrane Science*. Vol. 425–426, pp. 141-148. doi: <https://doi.org/10.1016/j.memsci.2012.08.004>
355. Waly T., Kennedy M. D., Witkamp G.-J., Amy G., Schippers J. C. (2011). Predicting and measurement of pH of seawater reverse osmosis concentrates. *Desalination*. Vol. 280, Is. 1–3, pp.27-32. doi: <https://doi.org/10.1016/j.desal.2011.06.057>
356. Alhseinat E., Sheikholeslami R. (2012). A completely theoretical approach for assessing fouling propensity along a full-scale reverse osmosis process. *Desalination*. Vol. 301, pp. 1-9. doi: <https://doi.org/10.1016/j.desal.2011.12.014>
357. Lee B.-S. (2015). Nuclide separation modeling through reverse osmosis membranes in radioactive liquid waste. *Nuclear Engineering and Technology*. Vol. 47, Is. 7, pp. 859-866. doi: <https://doi.org/10.1016/j.net.2015.08.001>
358. Kezia K., Lee J., Ogieglo W., Hill A., Benes N. E., Kentish S. E. (2014). The transport of hydronium and hydroxide ions through reverse osmosis membranes. *Journal of Membrane Science*. Vol. 459, pp. 197-206. doi: <https://doi.org/10.1016/j.memsci.2014.02.018>
359. Karakhim S. O., Zhuk P. F., Kosterin S. O. (2020). Kinetics simulation of transmembrane transport of ions and molecules through a semipermeable membrane. *Journal of Bioenergetics and Biomembranes*. Vol. 52, pp. 47–60. doi: <https://doi.org/10.1007/s10863-019-09821-8>
360. Peñate B., García-Rodríguez L. (2012). Seawater reverse osmosis desalination driven by a solar Organic Rankine Cycle: Design and technology assessment for medium capacity range. *Desalination*. Vol. 284, pp. 86-91. doi: <https://doi.org/10.1016/j.desal.2011.08.040>
361. Aghababaei N. (2017). Reverse osmosis design with IMS design software to produce drinking water in Bandar Abbas, Iran. *Journal of Applied Research in Water and Wastewater*. Vol. 7, Is. 1, pp. 314-318. doi: <https://doi.org/10.22126/ARWW.2017.776>
362. Park K., Burlace L., Dhakal N., Mudgal A., Stewart N. A., Davies P. A. (2020). Design, modelling and optimisation of a batch reverse osmosis (RO) desalination system using a free piston for brackish water treatment. *Desalination*. Vol. 494, 114625. doi: <https://doi.org/10.1016/j.desal.2020.114625>
363. Al-hotmani O. M. A., Al-Obaidi M. A. A., John Y. M., Patel R., Mujtaba I. M. (2020). An Innovative Design of an Integrated MED-TVC and Reverse Osmosis System for Seawater Desalination: Process Explanation and Performance Evaluation. *Processes*. Vol. 8, Is. 5, 607. doi: <https://doi.org/10.3390/pr8050607>
364. Srivastava S., Vaddadi S., Kumar P., Sadistap Sh. (2018). Design and development of reverse osmosis (RO) plant status monitoring system for early fault prediction and predictive maintenance. *Applied Water Science*. Vol. 8, 159. doi: <https://doi.org/10.1007/s13201-018-0821-8>
365. Husnil Y. A., Harvianto G. R., Andika R., Chaniago Y. D., Lee M. (2017). Conceptual designs of integrated process for simultaneous production of potable water, electricity, and salt. *Desalination*. Vol. 409, pp. 96-107. doi: <https://doi.org/10.1016/j.desal.2017.01.024>